Summer 2018

Developmental Steps for a Functional Three-Dimensional Cell Culture System for the Study of Asymmetrical Division of Neural Stem Cells

Martina Zamponi
Old Dominion University, martinazamponi98@gmail.com

DEVELOPMENTAL STEPS FOR A FUNCTIONAL THREE-DIMENSIONAL CELL CULTURE SYSTEM FOR THE STUDY OF ASYMMETRICAL DIVISION OF NEURAL STEM CELLS

by

Martina Zamponi
B.S. August 2017, Old Dominion University

A Thesis Submitted to the Faculty of
Old Dominion University in Partial Fulfillment of the
Requirements for the Degree of

MASTER OF SCIENCE

BIOMEDICAL ENGINEERING

OLD DOMINION UNIVERSITY
August 2018

Approved By:

Patrick Sachs (Co-Director)

Dean Krusienski (Co-Director)

Nicola Lai (Member)

ABSTRACT

Stem cells are a cell type present during and following development, which possess self-renewal properties, as well as the ability to differentiate into specific cells. Asymmetrical division is the cellular process that allows stem cells to produce one differentiated and one un-differentiated daughter cell during the same mitotic event. Insights in the molecular mechanisms of such process are minimal, due to the absence of effective methods for its targeted study. Currently, traditional methods of investigation include monolayer cell culture and animal models. The first poses structural limitations to the accurate representation of human tissue and cell structures, while animal models pose restrictions on the ability to visualize and manipulate the experiment performed, as well as being highly susceptible to error during data analysis and interpretation. Three-dimensional cell culture models are a novel approach to the study of cell mechanisms and disease, and are able to overcome many of the limitations of monolayer cell cultures and animal models.

It is our goal to devise a three-dimensional cell culture system suitable for the *in vitro* study of asymmetrical division of neural stem cells at a single cell resolution. Current methods based on the culture of cells embedded in extracellular matrix-derived substrates have been efficient tools for the understanding of cellular mechanisms. However, currently available three-dimensional cell culture systems lack important qualities for an efficient application to the study of asymmetrical division of neural stem cells. A defining quality of cells of the neural lineage is the generation of spontaneous electrical activity, necessary for the transmission of signals in the organism. Current systems lack the ability to perform electrophysiological measurements and characterize the functionality of the cells in culture. A second limitation is posed by the adoption of non-specific

substrates for cell culture able to recapitulate the natural cellular environment, as it is known that this has an impact on cell fate determination. Finally, current methods lack the ability to place and inject a controlled number of cells within the three-dimensional substrate, preventing the ability to perform studies at lower-cells resolutions.

In this project, I developed three Aims with the goal of overcoming the three major limitations of three-dimensional cell culture systems. In Aim 1, I evaluated the efficiency of Microelectrode Arrays systems to perform electrophysiological measurements of neural stem cells and neuronal networks *in vitro*. In Aim 2, I fabricated and characterized a porcine brain extracellular matrix-derived hydrogel, and I tested its ability to promote stem cells survival and proliferation. Finally, in Aim 3, I optimized the parameters of a custom 3D extrusion-based bioprinter to perform single cell and single beads resolution printing. Combined, the development of these Aims allowed me to lay the foundations for the development of a functional three-dimensional cell culture system applicable to the study of asymmetrical division in neural stem cells at a single cell resolution level, and which holds great potential for the uncovering of cellular mechanisms characteristic of stem cells and neurodegenerative disease.

This thesis is dedicated to my parents Brita Tomassoni and Claudio Zamponi.

A**cknowledgments**

Achieving the goals I set before me during the past year was not an easy task, and most importantly would not have been possible without all the support I have received by the people around me. I thank my family, because their efforts and sacrifices allowed me to focus on my studies and made my success in meeting the many deadlines of the past year possible; Dr. Patrick Sachs and Dr. Robert Bruno for welcoming me into their lab; my committee members Dr. Dean Krusienski and Dr. Nicola Lai; members of the laboratory Dr. Ross Petrella, Xavier Lewis-Palmer, Dr. John Reid; and Dr. Pete Mollica, whose patience, dedication, and friendship were essential.

TABLE OF CONTENTS

LIST OF ABBREVIATIONS

ABAM	Antibiotic-Antimycotic
cDNA	Complementary DNA
DAPI	4′, 6-diamidino-2-phenylindole
DCX	Doublecortin
DMEM	Dulbecco's Modified Eagle Medium
EB	Embryoid Body
EGF	Epidermal Growth Factor
ESC	Embryonic Stem Cell
FGF	Fibroblast Growth Factor
gDNA	Genomic DNA
GFAP	Glial fibrillary acidic protein
HCl	Hydrochloric Acid
ICC	Immunocytochemistry
IHC	Immunohistochemistry
iPSC	Induced Pluripotent Stem Cell
MAP2	Microtubule Associated Protein 2
MEA	Microelectrode Array
Ms	Mouse
NSC	Neural Stem Cell
PAGE	Polyacrylamide gel electrophoresis
PAX6	Paired Box Protein PAX-6

PBS	Phosphate-Buffered Saline
Rb	Rabbit
SDS	Sodium Dodecyl Sulfate
SOX1	SRY (sex determining region Y) box 1
SOX2	SRY (sex determining region Y) box 2
TBS	Tris Buffered Saline
Wt	Wild Type

LIST OF FIGURES AND TABLES

CHAPTER I – BACKGROUND

The goal of this study entailed the development of basic protocols to facilitate the study of targeted differentiation *in vitro*. Three aims were developed, and all contributed to the devising of an optimal method of investigation for asymmetrical division of neural stem cells in a three-dimensional environment. In aim 1, I tested the adoption of Microelectrode Arrays (MEA) for the functional characterization of neural stem cells and neurons. The ability of this technology to measure the real-time electrical activity observed in neural networks enables the study of changes in the electrophysiological properties of differentiating cells. In aim 2, I fabricated a porcine brain matrix-derived hydrogel suitable for cell culture, which allows for the study of asymmetrical division in a biomimetic environment. Lastly, in aim 3 I optimized a 3D extrusion-based bioprinter to obtain single cell/single beads resolution printing, to enable the study of asymmetrical division processes at a single cell resolution.

Stem Cells and Asymmetric Cell Division

Differentiation is the process that allows the generation of cellular diversity via the formation of specialized, terminally-differentiated cell types. It is characterized by an interruption of the cell cycle and the development of each cell's characteristic structures and functional properties [1]. The undifferentiated cells from which all the different types of somatic cells of the organism originate are known as stem cells. Based on their differentiation potential, which defines the diversity of cell types that they can subsequently generate, stem cells can be classified as totipotent, pluripotent, multipotent, oligopotent, and unipotent. Totipotent stem cells have the ability to divide and differentiate into any cells of an organism, including those found in the

extraembryonic tissue. This property allows for the formation of a developing embryo and the associated placenta after fertilization, all arising from a single totipotent cell. Pluripotency is defined as the ability of a cell to differentiate into another belonging to any of the three germ layers (endoderm, mesoderm, or ectoderm). Any fetal or adult cell can arise from pluripotent cells; however, they lack the ability to organize into an embryo [2]. Multipotent stem cells are found in developed tissue and can only generate cell types with specificity restricted to the tissue in which they are located, playing fundamental roles in organogenesis and regeneration. An example is provided by hematopoietic stem cells, responsible or the formation of the cell lineages circulating in the blood, or neural stem cells, responsible for the formation of neurons and the supporting glial cells present in the nervous system [2]. In contrast, oligopotent stem cells can only differentiate into a few, closely related cell types [3]. Finally, unipotent cells can only produce one cell type, but they are distinguished from normal cells because of their self-renewal properties, for which the cells can keep dividing over many generations [3]. However, the potency of cells is likely only understandable within the specific context of their microenvironment, as changing the location of a cell can drastically affect its differentiation potential [4, 5].

Two general categories in which stem cells can be classified are embryonic or adult stem cells, and their distinction resides in their preservation after the organism's development. Embryonic stem cells (ESC) can develop into any fully differentiated cell type of the body, and they are characterized by the properties of self-renewal and pluripotency [3]. They are found in the inner cell mass of the primordial embryo and are responsible for the generation of all the structures of the fetus [6]. Cells with the same properties as ESCs can be generated *in vitro* starting from somatic ones, and are known as induced pluripotent stem cells (iPSC) [7, 8]. This type of cell can be generated via the introduction of different combinations of transcription factors in the

differentiated cells. This can be accomplished by using viral vectors (such as lentiviruses or nonintegrating viruses), reprogramming factor mRNAs, micro RNAs, minicircle vectors, via transposons cloned into piggyBac vectors, or using episomal plasmids [9]. A first successful set of factors was identified by Yamanaka's group, and consisted of OCT3/4, SOX2, C-MYC, and KLF4, while a second combination was reported by the Thompson's group, and consisted of the reprogramming factors OCT3/4, SOX2, NANOG and LIN28 [4, 6-8]. The introduction of either combination of factors into mature cells, results in the activation of the genes associated with pluripotency and the induction of the adult cells from a mature, differentiated stage to an undifferentiated one.

Adult stem cells are found throughout various fully developed tissue and allow for tissue regeneration. Their location within the tissue is known as a stem cell niche, a concept first postulated by Schoefield in 1978. Here Schoefiled defined a "niche" as the *in vivo* microenvironment in which the cells are physically located and receive and exchange stimuli that influence their fate. These stimuli include cell-cell and cell-matrix interactions, and are responsible for the activation and repression of genes and transcription. They allow for the maintenance of stem cells in a quiescent state, in which division does not occur but the regular functioning of the cell cycle can be triggered by normal physiological stimuli, and the proliferative potential of the stem cells is preserved [10, 11]. Stem cell niches possess an intrinsic plasticity that allows them to coordinate the stem cells behavior in order to maintain the homeostasis of the tissue in which they are located [11, 12]. In fact, removal of cells from the niche, would result in loss of stemness and self-renewal capacity, as well as initiation of differentiation of the cells upon necessity [4, 13].

The mechanism that allows stem cells to maintain a state of self-renewal and at the same time maintain their potential to differentiate into mature cells, is known as asymmetric cell

division. Asymmetric division is defined as any division process that results in the formation of two daughter cells of different fates. Symmetrical division, results in the formation of two identical cells. Instead, stem cell asymmetric division creates two daughter cells directed towards different fates, a new stem cell and a differentiated one. This can be achieved through two main mechanisms: intrinsic or niche-controlled asymmetric cell division. In the first case, an axis of polarity is used during mitosis to ensure that self-renewal regulators are confined to only one half of the cell, thus consequently only one of the daughter cells will preserve its future-potency capabilities. In niche-controlled division, the fate of each daughter cell is determined by its position relative to the stem cell niche; also in this case, the orientation of the mitotic spindle during division plays a key role in the process. When the mitotic spindle is perpendicular to the niche, only one of the daughter cells remains in contact with it, preserving its pluripotency, while the second daughter cell will differentiate [14]. Alternatively, if the mitotic spindle is parallel to the stem cell niche, symmetrical division occurs and stem cells undergo self-renewal, demonstrating the key role that niches play in regulating stem cell potency and division.

Mechanisms of Study

The traditional methods of investigation to elucidate molecular mechanisms behind cellular processes and disease pathophysiology include either two-dimensional cell culture or animal models. Combined, they have been relatively efficient approaches assisting in the discovery of biological processes and the development of disease treatments. However, both techniques are flawed in that they do not provide for an accurate representation of the human *in vivo* cellular microenvironment.

Conventional two-dimensional cell cultures rely on the adherence of primary or immortalized cells on the culture dishes' flat surface, which provide the mechanical support needed by the cells. Culture of many different cell types is made possible by the ease with which nutrient media, optimized and supplemented with various exogenous components, can be delivered to the cells. Although characterization of the type and viability of cells, as well as simplicity of culture maintenance are easily achieved, cells in two-dimensional cultures lose their natural *in vivo* histological organization, leading to the inaccurate representation of tissues' structures. The loss of polarization observed in cultured cells may lead to alterations in their behavior and in the way in which cells and other extracellular components in culture interact. In fact, the histological organization of a tissue is strictly related to its function, and affects its biological functions and its biochemical specificities [15, 16].

In animal models, the inaccuracies encountered adopting monolayer cultures are overcome, as the cells and tissues studied are found in their natural disposition within the body. However, known and unknown differences between the animal physiology and the human physiology, are significant limiting factors in the accuracy of such approaches. The effectiveness of drugs and treatments has been shown to be species specific, with identical approaches producing discordant results when administered to animal models versus humans, and therefore reducing the reliability of results [17]. An additional risk factor in the adoption of animal models is the high probability of errors in the design of preclinical studies to accurately represent a disease population, as well as errors in the results' interpretation [18]. Finally, animal models often present limitation in the experimental design, as the use of live models allows for minimal visualization of the experiment progression, as well as a limit on manipulation opportunities.

A novel approach to the study of cellular mechanisms and disease, while maintaining a high degree of accuracy is represented by three-dimensional cell cultures. They overcome many of the structural limitations posed by monolayer culturing techniques and all the while reducing the error margin associated with the development and interpretation of studies in animal models. Different methods can be adopted to culture cells three-dimensionally, comprising of spheroid cultures, natural or synthetic scaffolds, cells sheets and hydrogels, the latter of which was chosen as model for the studies reported here. Three-dimensional cultures have so far revealed to be efficient means for the development and testing of drugs, for the study of the physiology of cells and cell populations, including their behavior and interactions, and have had applications in regenerative medicine research [19, 20]. Three-dimensional cultures have also been shown to promote the thriving of cell populations in culture. Their superiority to monolayer cell cultures resides in the cells' enhanced deposition of the ECM-components fundamental for cell movement and proliferation, as well as promoting integration of signaling pathways between cells, and ensuring a more natural response in drug studies [19, 20].

When considering an application to the study of asymmetrical cell division of neural stem cells *in vitro*, three-dimensional cultures represent an ideal approach, with some limitations. Physiological and functional measurements are retrieved with difficulty due to the typically random disposition of the cells in the system. Often, the substrates used for three-dimensional cell culture are not biomimetic, resulting in a system not accounting for the effect of different microenvironmental cues on the cell cultures' physiology and behavior. Finally, current systems are efficient for the formation and study of organoids, however they lack the ability to provide precise placement and dispensing of a limited number of cells, necessary for single-cell studies. These particular limitations were all approached in the development of the described project and

the devising of a functional system suitable for the study of asymmetrical division of neural stem cells.

A distinctive characteristic of cells of the neural lineage is their ability to produce spontaneous and evoked action potentials to transmit information. Traditional methods in the field of electrophysiology, such as patch clamp, rely on the analysis of the transmembrane voltages in isolated cells [21, 22]. Although they can grant a high level of accuracy even at single ionic channel resolution, these set-ups do not reflect the natural disposition of neural cells in networks, therefore not representing the behavior of cells in a population. Additionally, these methods are extremely invasive and the assays are usually terminal, as the cells cannot survive such procedures, and thus not allowing for the long-term culture and study of the cells in analysis [23]. Microelectrode arrays systems (MEAs) are a novel and efficient tool for the characterization of the electrophysiology of neural networks. They are constituted by a glass or plastic culture dish containing an array of electrodes in contact with the plated cells. These *in vitro* systems allow for the real time and simultaneous recording of spontaneous or evoked electrical activity of cells on multiple electrodes. The main advantage of this technology is the possibility to measure the activity of neural cells as part of a network rather than in single cells, more accurately representing the cell's natural disposition, in a very accessible way. This includes the performance of electrophysiological studies in the presence of both neurons and glial cells as well as accounting for the contact between different neurons. In addition, MEA plates allow for the long-term culture of stem and differentiated cells [23, 24]. This important quality enables the study of the variability in cells' electrophysiology associated with cell differentiation, development, and synchronization in a very controlled environment. MEA systems currently have a wide variety of applications, with particular focus on the study of the dynamics of neuronal signals and pharmacological studies.

This technology was applied to the development of my project, as it represents an optimal approach for the functional characterization of stem and neural cells populations.

The three-dimensional culture model used for this project envisioned cell cultures embedded in ECM-derived hydrogels. The substrates necessary to fabricate such hydrogels can be extracted from animal or human tissues. A first example is provided by Matrigel (Corning), a commercially available product extracted from the Engelbreth-Holm-Swarm (EHS) mouse sarcoma. This tumor is particularly rich in the type of proteins that constitute the basement membrane ECM, such as laminin, collagen IV, entactin, and different growth factors [25]. The Matrigel matrix is widely applied for the two-dimensional culture of stem cells as well as cells of the neural lineage. Additionally, the substrate has been applied to three-dimensional cultures for the study of neurodegenerative disease, as it promotes the survival of functional neurons and provides a structure that recapitulate the molecular characteristics of diseases such as Alzheimer's, more accurately than monolayer cultures [26-28]. Matrigel is the substrate predominantly adopted by research facilities, and it has proven efficient for the 2D and 3D culture of cells of the neural lineage. However, its tumor-origin and its unlikelihood of ever receiving FDA approval, and therefore being utilized in a clinical setting, raise concerns among researchers [29]. An alternative to the use of Matrigel is given by the extraction of the substrate directly from the animal or human tissues of interest. The process consists of extraction of the whole tissue and decellularization using a solution able to lyse the cells while preserving the extracellular matrix proteins intact. The decellularized product is then lyophilized, enzymatically digested and neutralized, in order to obtain a self-gelling product able to solidify upon warming into a hydrogel. This technique is currently employed in our laboratory, and substrates obtained from rat and human mammary tissues are manufactured for the study of the behavioral changes observed in breast cancer cell

lines cultured in a healthy environment and along normal mammary cells. Our laboratory has shown that tissue specific ECMs of the breast have unique properties in supporting the development of mammary epithelial cells [30]. Similarly, other laboratories have explored the use of tissue specific ECM for the culture of neural stem cells and neurons, demonstrating the possibility of manufacturing a substrate suitable for cell culture starting from animal brain tissue [31-33]. The adoption of a tissue-specific substrate derived from porcine brain was explored in this project, to devise a highly biomimetic 3D culture model.

A final limitation of traditional hydrogel-based 3D culture models is the ability to position and visualize a specific, limited number of cells within the hydrogels. This problem was approached in this project using a 3D extrusion-based bioprinter, which was developed in our lab as an adaptation of a relatively inexpensive, commercially available 3D printer [34]. It allows precise, coordinate-based, injection of variable concentrations of cells into substrates plated in standard-size culture plates, and allows the maintenance of cell viability after injection. The components critical to the development of this portion of the project were needle geometry, cell dilution concentration, medium, printing parameters, and the substrate adopted for the injection. Needle geometry plays a key role in the ability to dispense a minimum number of cells while avoiding structural damage. During the dispensing process, cells are subjected to many forces, and when their duration or intensity exceeds a certain threshold, disruption of the cellular integrity might occur. The shape of the needle influences the flow rate of the cells during dispensing as well as the level of damage inflicted to the cells. Through simulation and experimental models, it was possible to demonstrate that the least amount of damage is obtained adopting a tapered needle shape [34]. Additionally, the needle diameter is a fundamental parameter to consider while printing. A large needle tip allows for a greater number of cells to be released in a smaller amount

of time, and allows the passage of multiple cells at the same time. Smaller diameters, in the order of 150-500 μm, are more suitable for an application in single cell printing, as they are only wide enough to allow passage of a single cell, however such needles are more prone to clogging [34]. Cell dilution and printer parameters are two factors that need to be coordinated for the successful performance of single cell printing. The amount of solution extruded for each print can be adjusted to the cell concentration, and vice versa. When setting each one, it is important to determine an extrusion value suitable for the thickness of the substrate adopted, and limit the likelihood of the formation of cell clumps when determining the cell concentration. Lastly, the choice of substrate also affects the quality of the final print. The composition and stiffness of the hydrogel affect the type of deformation induced by the needle penetration. Stiffer gels are less plastic and tend not to deform to properly adapt to the volume of cells injected while preventing permanent deformation. It is then important to consider the structural behavior of the substrate when placed in different culture plates. Specifically, adhesive forces between the substrate and the cultureware result in the formation of a meniscus in correspondence with the hydrogel surface. Steepness of the meniscus is dependent on the material adopted and the quantity of substrate applied relatively to the height and width of the wells in the chosen culture plate. Minimizing the meniscus size is fundamental to ensure continuity in the printing process. Additionally, when the printing is performed envisioning culturing of the printed cells, the substrate of choice must be biocompatible with the type of cells adopted. All the parameters described were considered and adjusted in order to enable single-cell printing, and ultimately allow for the study of neural stem cell asymmetrical division at a single-cell resolution.

Project Aims

The overall goal of this research project is the development of the basic protocols necessary for a functional three-dimensional culture system. Specifically, such system was conceived for an application in the study of asymmetrical division in neural stem cells. Three separate aims were envisioned to ensure the development of the different qualities of the system, and were (1) the adoption of microelectrode arrays (MEA) systems for the functional characterization of neural stem cells and neurons, (2) fabrication of porcine brain matrix-derived hydrogels suitable for cell culture and (3) optimization of a 3D extrusion-based bioprinter to obtain single cell/single beads resolution printing.

Aim (1) – Adoption of Microelectrode Arrays (MEA) systems for the functional characterization of neural stem cells and neurons.

Microelectrode Arrays systems are a novel technology that allows for the real-time characterization of the spontaneous and evoked electrical activity of excitable cells. The placement of multiple microelectrodes in contact with the cells of a population in culture enables the simultaneous measurement of voltage changes in multiple regions of the same cell population. MEAs system represent an ideal approach for the study of the electrophysiology of neural stem cells and neurons in long-term cultures, with the possibility to focus on events such as development, potentiation, depression and synchronization.

The first aim of this project focused on the application of an MEA system for the functional characterization of neural stem cells and neurons. The long-term goal of this research envisions the development of a three-dimensional culture system and, consequently, of an appropriate method for the functional characterization of cells in such structure. Being able to assess the

functionality of a two-dimensional neural culture represents the first step towards the progression of this project.

Aim (2) – Fabrication of porcine brain matrix-derived hydrogels suitable for cell culture.

A common approach to 3D culture, is through the fabrication of protein-derived hydrogels. Many of such models have been designed using extracted substrates, such as extracellular matrix (ECM), which possess similar, although not exact, properties as the corresponding *in vivo* environment. The cellular microenvironment plays a role in directing cell fate [4, 5, 30], therefore being able to mimic the natural cellular microenvironment allows a high level of accuracy of the devised models, both under the structural aspect as well as the behavior of cells in culture.

The second aim of the project focused on the adaptation of existing ECM isolation protocols for the fabrication of a substrate derived from porcine brain extracellular matrix, suitable for two- and three-dimensional culture of neural stem cells and neurons. Such structure represents the ideal method of culture of neural cells in order to mimic their natural environment and three-dimensional disposition, with potential applications in the study of neural cells mechanisms typical of normal and disease conditions.

Aim (3) – Optimization of a 3D extrusion-based bioprinter to obtain single cell/single beads resolution printing.

Asymmetric division is a subject of research that has long been explored, but the limited theoretical knowledge behind the possible mechanisms that drive it represents a great limiting factor with regard to the performance of practical experiments. Insights into the dynamics of the process have been partially unveiled by Habib et al., who demonstrated the capability to induce

asymmetric division in a pluripotent stem cell model upon contact with Wnt transcription factor [35]. The experiment was conducted utilizing mouse embryonic stem cells cultured along Wnt3a or Wnt5a-conjugated to microbeads, and the authors were able to observe that contact with the beads allowed preservation of self-renewal properties of stem cells instead of inducing differentiation. The setup of this experiment allowed the observation and distinguishing of differentiated vs. non-differentiated products of asymmetric division, but prevented the performance of any study during or following division. The last aim of this project consisted in the optimization of a 3D extrusion-based bioprinter, with the goal of obtaining single cells and single WNT conjugated beads injected in different substrates, to be later applied to the study of asymmetric division at a single cell resolution, following the model proposed by Habib et al.

Research Significance

The ability of a model to faithfully mimic the characteristics of a physiological system is a fundamental quality for its application in translational research. Monolayer culture systems and animal models, although widely adopted for the study of stem cells and asymmetric division, present significant limitations. Three-dimensional culture models hold great potential in the field, as they can be devised to reproduce the physiological conditions of a system, both under the structural and biochemical point of view. The development of the described project lays the foundations of a 3D culture system ideal for the culture and study of stem and neural lineage cells. This system holds great potential in research in the field of stem cells and neurodegeneration. Combined, the real-time physiological measurements obtained through MEA systems, the use of a highly biomimetic tissue-specific substrate, and the use of precise 3D extrusion-based bioprinting, grant an unprecedented level of accuracy in the study of neural stem cell asymmetrical division and differentiation. Further, this system allows for a more precise study of molecular

mechanisms of neurodegenerative disease, as well as higher expected efficiency in the development and testing of potential treatments.

CHAPTER II – MATERIALS AND METHODS

a. Aim (1) – Functional Characterization of Neural Stem Cells and Neurons

Induced Pluripotent Stem Cells Generation and Culture

One wild-type iPSC-Wt, two Huntington's disease affected iPSC-GM02191 (iPSC-HD1) and iPSC-GM04022 (iPSC-HD2), and one Alzheimer's disease iPSC-AG09088 (iPSC-AD) induced pluripotent stem cell lines, were previously generated in our lab starting from human fibroblast lines. Huntington's and Alzheimer's diseased cells were purchased from Coriell Cell Repositories (Camden, NJ). Briefly, cellular reprogramming and validation was conducted using the CytoTune™ – iPS 2.0 Sendai Reprogramming Kit (Life Technologies, Carlsbad, CA) [36]. Following successful reprogramming, the cells were cultured under feeder-dependent conditions on irradiated murine-embryonic fibroblasts (iMEFs) (GlobalStem; Gaithersburg, MD). iPSC lines were initially cultured in complete KnockOut Serum medium (KOSR), constituted by KnockOut™ Dulbecco's Modified Eagle's Medium (DMEM)/F-12 medium (Life Technologies), supplemented with 20% KnockOut™ Replacement Serum, 1x MEM Non-Essential Amino Acids (Life Technologies), 10 ng/mL of Basic Fibroblast Growth Factor (Life Technologies), 55 nM β-mercaptoethanol, (Sigma Aldrich; St. Louis, MO) and 1% Antibiotic-Antimycotic (ABAM; Thermo Fisher Scientific, Whaltam, MA). Medium was completely replenished daily. Upon reaching of an adequate size, as determined following the Maintenance of Human Pluripotent Stem Cells in mTeSR™1 technical manual (STEMCELL Technologies; Cambridge, MA), the colonies were manually split and passaged for expansion. iPSC lines were then adapted to a feeder-independent protocol using Geltrex® LDEV Free hESC-qualified matrix (from here on referred as Geltrex®) (Thermo Fisher Scientific) coated culture plates. The iPSC lines were then cultured with mTeSR™1 medium, composed by mTeSR™1 Basal Medium (STEMCELL Technologies),

5x mTeSR™1 Supplement (STEMCELL Technologies) and 1x ABAM. Subsequent passages were performed upon adequate growth of the colonies and pluripotency expression, verified, respectively, following the directions provided by the Maintenance of Human Pluripotent Stem Cells in mTeSR™1 technical manual, and with positive staining for TRA-1-60 (Life Technologies) performed according to the manufacturer's protocol. Passages were performed manually or using the StemPro® Accutase® Cell Dissociation Reagent (Thermo Fisher Scientific).

Neural Stem Cells Induction and Culture

Neural stem cell (NSCs) lines were obtained for each of the previously described iPSC lines using the STEMdiff™ Neural System Embryoid Body (EB) protocol (STEMCELL Technologies). iPSCs adapted to feeder-independent conditions and cultured in mTeSR™ 1 medium were plated on an Aggrewell™ 800 plate, and cultured in STEMdiff™ Neural Induction medium (STEMCELL Technologies). Daily partial (3/4) medium change was performed from Day 1 – 4. On day 5 the EBs were harvested from the Aggrewell™ 800 wells and re-plated on Geltrex®-coated culture plates. All NSC cultures from this point were maintained on culture plates coated with Geltrex® matrix at a 1:100 dilution. Daily full medium change was performed until Day 11. On Day 12 the newly formed neural rosettes were selected using the STEMdiff™ Neural Rosette Selection Reagent (STEMCELL Technologies). Cells were cultured in STEMdiff™ Neural Induction medium until ready for passage 1, approximately day 19. NSC outgrowths formed between the rosette clusters, and passage 1 was performed when confluency reached 80-90%. Passage was performed using TrypLE™ Express Enzyme (1X) (Thermo Fisher Scientific) as recommended by the manufacturer. Cells were cultured in complete StemPro® NSC Serum Free Medium (Thermo Fisher Scientific), composed of KnockOut™ DMEM/F-12 medium, StemPro®

Neural Supplement 50X (Thermo Fisher Scientific), FGF-basic (AA 10-105) Recombinant Human (Thermo Fisher Scientific), EGF Recombinant Human (Thermo Fisher Scientific), 1X GlutaMAX™ (Thermo Fisher Scientific), and 1X ABAM. Media was replenished completely every other day. The identity of the NSCs obtained with the neural induction protocol was confirmed through immunocytochemistry staining for the antigens listed in Table 1 as described below.

Neuronal Differentiation

General neuronal differentiation was performed using previously published protocols [37, 38]. NSCs were cultured in complete StemPro® NSC Serum Free Medium until 90-100% confluency was achieved. Successively the culture medium was substituted with Neurobasal™ Medium (Thermo Fisher Scientific), supplemented with 2% B-27™ Supplement (50X) (Thermo Fisher Scientific), 0.5 mM GlutaMAX™, 1X ABAM, 500 nM puromorphamine (STEMCELL Technologies), 50 nM retinoic acid (STEMCELL Technologies). Partial (1/2) medium change was performed daily, limiting the direct exposure of the differentiating cells to air during the process. Immunocytochemistry was performed at Day 15 of differentiation (as described below), and the molecular markers tested to confirm the identity of the maturing neurons are listed in Table 1.

Immunocytochemistry

Immunocytochemistry assays were performed to confirm the identity of newly generated neural stem cell lines, as well as to test the efficiency of our neuronal differentiation protocol. Samples were washed twice in 1X tris-buffered saline (TBS) for 5 minutes each – all the subsequent washes were performed for the same amount of time – and fixed in 10% formalin

(Thermo Fisher Scientific) for 20 minutes. Samples were then washed with 1X TBS three times, incubated with 0.1% NP40 in TBS at room temperature for 10 minutes, and then blocked with 10% goat serum for 60 minutes. Primary antibodies were diluted in 1% goat serum according to the manufacturer's instructions, and following application they were incubated overnight at 4°C. Next, after washing the samples with TBS four times, Alexa Fluor™ 488 and 568 secondary antibodies (Thermo Fisher Scientific) diluted 1:1000 in 1% goat serum were added and the samples were incubated in the dark, at room temperature, for 60 minutes. Samples were newly washed in TBS four times, and nuclear stain was performed adding DAPI diluted 1:1000 in 1% goat serum. The samples were finally washed four times in TBS, and images were acquired with a Zeiss Axio microscope with a short-working distance 20X objective.

Nucleic acid extraction and gene expression analysis

The identity of the newly formed neural stem cell lines was confirmed analyzing their relative expression of genes of interest, listed in Table 1. Gene expression data were obtained through RNA extraction and purification, cDNA synthesis, and Real-Time quantitative PCR assays.

Upon reaching of the appropriate confluency level of the cultures, RNA extraction was performed using TRIzol® (Thermo Fisher Scientific) reagent following the manufacturer's protocol. The RNA phase was isolated through centrifugation. Next, the RNA was precipitated using 100% isopropanol, and washed using 75% ethanol. Finally, the isolated RNA was resuspended in 22 µL of nuclease-free water. Purity of the RNA samples was ensured by the performance of gDNA digestion using Deoxyribonuclease I, Amplification Grade (Thermo Fisher Scientific), following manufacturer's protocol. RNA was then quantified using a NanoDrop 2000

(Thermo Fisher Scientific), and its concentration was determined based on the UV absorbance levels at 260 nm (A260 nm). Quantification values were considered acceptable with 260/280 ratios >1.7, and 260/230 ratios > 1.8. The RNA product was then used to synthesize cDNA strands using the High Capacity cDNA Reverse Transcription Kit (Thermo Fisher Scientific), as per manufacturer's protocol.

cDNA samples were amplified using TaqMan® Gene Expression Assay (Applied Biosystems) to quantify the original mRNA levels. Optimized primers and probes were provided for the specific target genes in analysis, and each probe presented a 5' terminal reporter dye FAM (6-caroxyfluorescein) and a 3' terminal non-fluorescent quencher dye (NFQ-MGB). To perform the amplification, real-time quantitative PCR assays were performed using a StepOnePlus™ Real-Time PCR System (Applied Biosystems; Foster City, CA). Complete samples for the reactions comprised 1X TaqMan® Fast Advanced Master Mix, 1X TaqMan® Gene Expression Assay, and 50 ng of cDNA template, for a total final volume of 20µL. All PCR experiments comprised a total of 40 thermal amplification cycles, and each cycle consisted of 1 cycle of 2 minutes at 50°C, 1 cycles of 20 seconds at 95°C, and 40 cycles of 1 second at 95°C and 20 seconds at 60°C. All experiments were performed in triplicates, and each sample was sub-sampled three times, to ensure statistical significance of the results. Gene expression analysis was conducted using the $2^{-\Delta\Delta Ct}$ of the average Ct for each subsample. Statistical analysis and data graphical representation were performed with Prism 7 (GraphPad Software; La Jolla, CA).

Table 1.

Neural lineage related proteins targeted during characterization of neural stem cells and neurons.

Target	Marker	Description	Brand	Catalog No.	Anti
Doublecortin / DCX	Neuron	Cytoplasmic protein that regulates the organization and stability of microtubules, directing movement of cortical neurons during development.	Life Technologies	481200	Rb
GABA B1	GABA Neuron	Targets cells presenting GABA receptors. Mainly found secreted and in brain cells' membranes.	ABCAM	ab55051	Ms
GAD65/67	GABA Neuron	Associated with neuronal presynaptic clusters and cytosolic leaflets of Golgi membranes.	ABCAM	ab11070	Rb
GFAP	Astrocyte	Associated with intermediate filament in CNS cytoplasm. Distinguishes astrocytes from other glial cells.	ABCAM	ab10062	Ms
MAP2	Neuron	Microtubule Associated Protein 2. Involved in microtubule assembly during neurogenesis.	Thermo Fisher Scientific	MA5-1282C	Ms
Nestin	Neural Stem Cell	Intermediate filament protein expressed during dividing and developing cells.	Thermo Fisher Scientific	MA1-110	Ms

OLIG	Oligodendrocyte	Oligodendrocyte-specific protein. Fundamental to ensure cell-cell adhesion in tight junctions.	ABCAM	ab53041	Rb
PAX6	Neural Stem Cell	Transcription factor involved in the development of CNS cells	Thermo Fisher Scientific	MA1-109	Ms
SOX1	Neural Stem Cell	Transcriptional activator located within the nucleus of developing CNS cells (NSCs). Associated with cell's multipotency and pluripotency.	ABCAM	ab87775	Rb
SOX2	Neural Stem Cell	Required for stem cell maintenance in the CNS	Thermo Fisher Scientific	PA1-094	Rb
Tyrosine Hydroxylase (TH)	Neuron	Expressed in brain and adrenal glands. Characterizes adrenergic neurons	ABCAM	ab112	Rb
Beta III Tubulin (TUJ1)	Neuron	Major constituent of microtubules. Found mainly in PNS and CNS axons.	ABCAM	ab18207	Rb

Microelectrode Arrays System and Set Up

Functional characterization of neural stem cells and neurons was performed in collaboration with the Neural Engineering Lab at George Mason University. Electrical activity of the cell networks was measured using an MEA1060-Inv-BC (Multichannel Systems, Reutlingen,

Germany) amplifier and filter system with 1,200 total gain and band pass filter from 300 to 3k Hz. This setup allowed for single-well recording, and the MEA plated used presented 60 recording electrodes each. The software MEA_Select V1.3.0 (Multichannel Systems) was used to select the electrodes for recording and for grounding. Temperature control was achieved with a heated surface placed underneath the recording device, and set to about 35°C, using the TCX-control V1.3.4 software (Multichannel Systems). Signal visualization and analysis was possible through the software MC_Rack V4.5.10 (Multichannel Systems), which allowed visualization of the raw signals as well as the extracted wavelengths.

Plating of MEAs

Single wells were plated with neural stem cells and neurons following two distinct protocols, and their efficiencies were tested and compared. Plates were first coated on their entire surface with Geltrex® matrix diluted 1:100 in DMEM/F-12. Neural stem cells were plated and cultured in complete StemPro® NSC Serum Free medium, replenished every other day, until 80-100% confluency was reached. Neuronal differentiation was conducted directly on MEA plates, and was initiated in selected plates upon reaching of confluency of the NSCs by switching to neural differentiation medium, partially replenished daily. Alternatively, MEA plates were coated with 0.1% Poly-L-Lysine (Sigma Aldrich) and laminin (Sigma Aldrich). Poly-L-Lysine solution was used to cover the center of the MEA plates and incubated for 5 minutes at room temperature. The excess solution was aspirated and a 20 µg/mL solution of laminin in sterile water was used to cover the electrodes. Neural stem cells and 3-weeks-old neurons, previously differentiated in Geltrex®-coated cultureware, were plated onto the MEA plates. The cell lines used for these electrophysiological studies were Wt, and GM04022 (Huntington's disease).

Data collection and analysis

Spike selection from the raw data obtained using the MEA1060-Inv-BC amplifier was done using a -5-standard deviation threshold. Spontaneous electrical activity of NSCs and neurons was recorded for 5 minute intervals for 5 consecutive days, with media replenished after each recording. After collection of this first set of data, neuronal differentiation was induced in the MEA plates seeded with NSCs and 5 minute recordings of their spontaneous electrical activity were collected every other day. After recording, the raw data was analyzed using the Offline Sorter (Plexon Inc., Dallas, TX) software, which allowed for spike isolation and waveform extraction. This type of analysis enabled us to determine the number of spiking neurons acting on each electrode and visualize their distinct action potential shape. Further analysis was conducted using a custom Python script to construct raster plot of the activity of the neural networks. Such graphs enable the visualization of the spiking activity recorded on all the functioning electrodes relatively to their occurrence during the recording interval.

b. Aim (2) – Fabrication of porcine brain matrix-derived hydrogels suitable for cell culture

Brain tissue origin and extraction

Tissue was extracted from adult animals and obtained from three sources. Two frozen porcine heads were purchased from Central Meats & Almost Catered (Chesapeake, VA). Two heads were provided by Dr. Christian Zemlin at the Frank Reidy Center for Bioelectrics, after the animals were sacrificed for the research purposes of his laboratory. Finally, two heads were purchased from Animal Biotech Industries, Inc (Danboro, PA).

All brain tissues were extracted in our laboratory immediately after acquisition or upon complete thawing. The skullcap was carefully removed to preserve the intact brain structures at best. Cerebrum, cerebellum, pons, midbrain, medulla, and part of the spinal cord and optic nerves were collected. The blood brain barrier, the meninges layers, and the blood vessels were carefully removed, and the tissue was washed with sterile water to remove residual blood.

Hydrogel formation protocol

Following extraction and wash, the brain tissue was cut into sections and washed in a 2% v/v solution of N-Lauroyl Sarcosine (NLS) sodium salt solution (Sigma Aldrich) and 2X ABAM. This and all subsequent washes were performed at room temperature in a temperature controlled orbital shaker (MaxQ 4000; Thermo Scientific). The solvent allowed for removal of the cells from the tissue inducing lysis, while maintaining the extracellular matrix proteins intact. The decellularization solution was replaced every 24 hours for 4-7 days (depending on the relative size of the tissue samples), until complete cell removal. The product was then transferred into high-speed autoclavable centrifuge tubes, and centrifuged at 17,500 x g for 5 minutes. The supernatant was carefully decanted to prevent loss of ECM, and the product was resuspended and rinsed in ultra-pure water. A total of ten washes were performed to ensure complete removal of the NLS solvent. Subsequently, the product was washed once in isopropyl alcohol (IPA) for 24-48 hours to remove any lipid component. Finally, the product was washed an additional ten times with ultra-pure water to remove any residual IPA. The decellularized tissue was then lyophilized using a FreeZone Triad Freeze Dryer (Labconco; Chapel Hill, NC). Successively the product was mechanically homogenized using liquid nitrogen. The ECM was then solubilized though an enzymatic digestion process, a 1 mg/ml solution of pepsin from porcine gastric mucosa (Sigma

Aldrich) in 0.1 M HCl was prepared and stirred overnight at 4℃, and the product was diluted 20mg:1mg of pepsin. The solution's pH was adjusted to about 1.5 using 0.1M HCl, and allowed to digest for 24-48 hours. This process results in an acidic product, and dialysis was used to neutralize the digested solution. A 6-8kDa dialysis tubing (Spectra Por; Spectrum Labs, Virginia Beach, VA) was used to dialyze the product:pepsin solution against a neutral PBS solution, a procedure performed at 4°C to prevent premature gel formation. The product obtained was self-gelling when kept above 4-8°C. Hydrogels were prepared placing a set volume of product in the appropriate container, and incubating at 37°C for two hours.

Decellularized Tissue Characterization: Immunohistochemistry

Native and decellularized brain tissue were characterized to define the efficiency of the decellularization protocol. Samples from the unprocessed cerebrum, cerebellum, pons, midbrain and medulla, and unidentified samples of decellularized tissue were fixed in 10% formalin for two hours and then preserved in 70% ethanol. The fixed samples were embedded in paraffin and sectioned at the EVMS Histology Laboratory (Eastern Virginia Medical School, Norfolk, VA). One section of each sample was stained with hematoxylin and eosin to define their nuclear content, while the remaining ones were utilized for immunofluorescence assays and tested for various cell markers. For each immunohistochemistry (IHC) assay, sections were washed twice in xylenes (Thermo Fisher Scientific) for 8 minutes each, to remove the paraffin from the slides. Sections were rehydrated doing two 2 minutes washes in 100% ethanol, one 1-minute wash in 90% ethanol, one 1-minute wash in 70% ethanol, and one 1-minute wash in distilled water. Slides were rinsed in 1X TBS and transferred to preheated citrate buffer (antigen retrieval buffer) for 25 minutes. After cooling, the samples were rinsed twice in 1X TBS and washed in the same solution until

cool. Samples were blocked with 10% goat serum and incubated for 60 minutes, at room temperature, in the dark. Primary antibodies were diluted in 1% goat serum according to the manufacturer's instructions, placed on the slides, and incubated overnight in humidified chambers, at 4℃. A negative control was performed by addition of 1% goat serum only. Cell markers chosen for analysis with their specific targets are summarized in Table 1. Next, slides were rinsed twice, and successively washed thrice in 1X TBS. Secondary antibodies were diluted 1:1000 in 1% goat serum, applied to the samples and incubated at room temperature, in the dark, for 60 minutes. Slides were washed with TBS and nuclear stain DAPI, diluted 1:1000 in 1% Goat Serum, was applied, and the samples were incubated for 5 minutes protected from light. Samples were finally washed thrice in 1X TBS and images were acquired with a Zeiss Axio Observer microscope at 10X or 20X magnification.

Decellularized Product Characterization: genomic DNA content

The genomic DNA (gDNA) content of the native and decellularized brain tissue was extracted, purified and quantified to determine the efficiency of our protocol. Extraction of the genetic material was performed with the DNeasy® Blood and Tissue Kit (Qiagen; Hilden, Germany) on unprocessed samples of cerebrum and cerebellum and decellularized samples of unidentified porcine brain tissue. The total DNA purification was performed according to the manufacturer's protocol for extraction from tissues.

Between 15 – 25 mg of tissue were placed into eppendorf tubes, Buffer ATL and proteinase K were added, and the samples were incubated at 56°C until complete lysis of the tissues. AL buffer and ethanol were successively added to the tubes and mixed thoroughly, and samples were transferred into DNeasy Mini spin columns. A first spin at 6000 x g was performed and the flow

through was discarded, next AW1 Buffer was added to the sample and the centrifugation step was repeated.

Isolated gDNA samples were concentrated and purified with 100% ethanol and sodium acetate and resuspended in 20 µL of nuclease-free water. gDNA concentration was quantified using a Nanodrop 2000, and purity of the samples was deemed acceptable with 260/280 ratios around the value of 1.8.

Hydrogel Product Characterization: DC™ Protein Assay

The total protein concentration of the final product was evaluated with a DC™ Protein Assay (Bio-Rad Laboratories, Portland, ME), performed as per manufacturer's instructions. To perform the colorimetric assay, five serial dilutions of a bovine serum albumin protein standard (Bio-Rad Laboratories) were prepared, as well as five dilutions of the brain-derived hydrogel, to ensure that the protein concentration in the product fell within the concentrations of the protein standard. Product concentration was measured spectrophotometrically using a Nanodrop 2000 and a wavelength of 750 nm.

Hydrogel Product Characterization: Polyacrylamide Gel Electrophoresis

Qualitative characterization of the hydrogel product was done performing polyacrylamide gel electrophoresis (PAGE) and detection was achieved through coomassie 250 staining.

A 7.5% polyacrylamide gel (Bio-Rad) was inserted in a vertical electrophoresis cell (Bio-Rad Laboratories), and the cell's chambers were filled with 1X SDS Buffer, to obtain a continuous buffer system. Samples were prepared as serial dilution of the product, from 100% to 6.50% concentration of product to sterile water. Geltrex® matrix diluted 1:100 in sterile water, for a final

concentration of 1.57 µg/µL, was used to compare the protein content of brain-derived matrix to the commercially available product. Samples were diluted with laemmli buffer to form a 1X solution, heated to about 100°C and incubated for 10 minutes, and equal amounts of each sample were loaded into the polyacrylamide gel wells. The gel was resolved applying voltage at 5 V for five minutes, and then at 100 V until the ladder sample reached the lower portion of the gel.

After completion of PAGE, the polyacrylamide gel was carefully removed from the chamber and washed with deionized water. A coomassie G-250 stain was prepared with 50% methanol, 10% acetic acid, 40% deionized water and 0.5% of coomassie brilliant blue G-250 dye (Amresco, Solon, OH), and used to wash the gel for 5 minutes. Successively, the gel was rinsed with deionized water, and a destain solution composed of 40% methanol, 10% acetic acid and 50% deionized water was applied overnight, until visible bands appeared on the gel. Imaging of the stained gels was performed with a myECL™ Imager (Thermo Fisher Scientific),

Cell Culture and Biocompatibility

The suitability of the hydrogel products for cell culture purposes and their biocompatibility were tested to establish the potential application of this technology in future translational research projects. Suitability of the products for use in the laboratory was tested by using the hydrogels to coat cultureware and successively seed it with neural stem cells. Plastic cultureware was coated with a 0.1% poly-L-lysine solution (Sigma Aldrich) according to manufacturer's protocol. The brain-derived product was diluted 1:100 in DMEM/F-12 or acetic acid, plated over the dried laminin layer and incubated overnight at 37℃. Next, wild-type NSCs were seeded on the culture plates and cultured as previously reported (1).

In vivo injections of the brain-derived matrix were performed in rats to assess its biocompatibility, and injected with human wild type NSCs and iPSCs to determine its ability to promote cell survival, proliferation, and differentiation. The endogenous epithelium of the inguinal mammary glands of sedated 3 week old mice was removed, the brain-derived product was diluted 1:2 in DMEM/F12 and injected into the cleared mammary fat-pad. Consequently, 200,000 cells of either line were injected in the gel. Cells were also injected in the rats' mammary gland in absence of the brain-derived matrix, to provide a negative control. After ten weeks of incubation, the tissue was removed, fixed and embedded in paraffin for further analysis.

c. *Aim (3) – Optimization of a 3D extrusion-based bioprinter to obtain single cell/single beads resolution printing.*

Cell lines and culture

For the development of the third aim of this project, three breast-epithelial cell lines were utilized. The lines MCF-12A, MCF-7, and MDA-MB-468 were previously acquired from American Type Culture Collection (ATCC). Cells of the MCF-12A line were previously transfected in our laboratory to express the RFP protein, while those of the MCF-7 and MDA-MB-468 were transfected to express GFP protein. The three cell lines were adopted for the third aim of this project based on their availability in the lab, ease of culture, ease of visualization after printing, and elevated proliferation rates. MCF-7 and MDA-MB-468 were cultured in DMEM containing GlutaMAX^{TM} complete medium supplemented with 10% fetal bovine serum (Life Technologies) and 1X antibiotic-antiomycotic. MCF-12A cells were cultured in DMEM/F-12 with GlutaMAX^{TM}, supplemented with 5% horse serum (Thermo Fisher Scientific), 20 ng/mL hEGF (Thermo Fisher Scientific), 10 µg/mL bovine insulin (Sigma Aldrich), 500 ng/mL hydrocortisone (Sigma Aldrich),

and 1X ABAM. All cells were cultured at 37℃ in a 5.0% CO_2 incubator, and media was replenished every 2-3 days. Upon reaching of 80-100% confluency cells were passaged using TripLE® Express enzyme, following the manufacturer's protocol.

Bioprinting System

A custom-made 3D extrusion-based bioprinter was previously developed in our laboratory by modifying a commercially available model, Felix 3.0 (FELIXrobotics, NL) [34]. Needles were manufactured prior to each print using a Model P-1000 Flaming/Brown Micropipette Puller (Sutter Instruments; Novato, CA), and the needle diameter was adjusted to fall in the range of 100-500µm.

Single cell/single beads resolution prints were obtained through progressive experiments, in which printer parameters and materials chosen were varied and adjusted. Initial experiments were performed using one single cell line, with the goal of achieving single-cell printing resolution. The substrates adopted were hydrogels constituted of 1% agarose diluted in deionized water, and chosen for its accessibility, and suitability for extrusion-based printing [39]. Prints were performed in 24-well culture plates, and each well contained 500 µL of agarose hydrogel, a volume chosen to minimize the meniscus size and ensure consistency within the same print. The initial concentration of cells was arbitrarily set to a value of 300,000 cells/mL. Cells were digested using TripLE® Express enzyme according to the manufacturer's protocol, and resuspended in 1% EDTA solution, to maintain the single-cell state after resuspension and prevent the formation of cell clumps during printing. Extrusion values were progressively adjusted and optimized to a value e=0.009 to obtain single-cell prints.

After achievement of single-cell resolution on agarose hydrogel in 24-well plates, prints were performed on PEN slides with the same objective. Slides were coated with approximately 2

mL of 1% Agarose gel, and the same parameters were maintained to perform the prints and obtain single cell resolution.

The aim of the experiments was then adjusted to achieve single cell/single bead resolution printing. To one ml of cells diluted to a concentration of 300,000 GFP labeled-cells/ml were added 0.5µL of red FluoSpheres® Fluorescent Microspheres (Thermo Fisher Scientific) diluted 1:1000. Prints were performed on PEN membranes coated with 1% Agarose gels or Corning® Collagen I, High Concentration, Rat Tail (Corning; Corning, NY). The gels were prepared to a final product concentration of 1.2 mg/ml. A volume equal to 2.3% of the Collagen I stock needed of 1N sodium hydroxide was added to the stock product, and then 1X PBS and 1X DMEM were added to reach the final desired volume.

Qualitative and quantitative analysis of prints

Resolution of the prints was evaluated qualitatively and quantitatively. Upon performance of each printing experiment, samples were visually inspected using a Zeiss Axio Observer microscope at 10X magnification, to establish presence of single cells or single beads. Printing resolution was quantified through nuclear staining, using DAPI diluted 1:1000. Percentage of single cell prints in one experiment was calculated upon visual inspection.

CHAPTER III – RESULTS

a. Aim (1) – Functional Characterization of Neural Stem Cells and Neurons

In the first portion of this project, I aimed at testing the suitability of Microelectrode Array systems for the functional characterization of neural stem cells and neurons. First of all, I generated neural stem cell lines starting from wild-type, Alzheimer's disease, and Huntington's disease induced pluripotent stem cell lines (iPSC). To do so, I cultured iPSC lines, and after confirming the pluripotency of the colonies I performed the previously described neural induction protocol to generate NSCs lines, and I characterized their identity through immunocytochemistry assay. I then chose a neuronal differentiation protocol, performed the neuronal differentiation of the various NSCs lines, and confirmed the identity of the maturing neurons through immunocytochemistry staining. These preliminary experiments were fundamental for the development of the cell types and cell lines required for the development of the first aim, and which can be adopted for further studies concerning asymmetrical division of neural stem cells and neurodegenerative disease.

Efficiency of Cell Culture, Induction and Differentiation Protocols

Induced pluripotent stem cells are characterized by their ability to self-renew and also differentiate into any cell type. Pluripotency of iPSC lines was confirmed through TRA-1-60 live staining, a pluripotent specific marker. Colonies stained positively both on feeder and feeder-free conditions, while MEFs and Geltrex® matrix did not stain (Figure 1). This confirmed the identity of the iPSC colonies, and their suitability to be applied for the generation of cells of the neural lineage.

To begin the process of neural differentiation, select iPSC colonies were replated on an Aggrewell™ 800 plate, and the STEMdiff ™ Neural System Embryoid Body (EB) protocol was

followed to induce the formation of embryoid bodies, neural rosettes and, finally, neural stem cells colonies (Figure 2). Efficiency of the neural induction protocol was tested through immunocytochemistry staining assays. The control NSC wild type line (NSC-wt; bASC3.2), the NSC Alzheimer's disease line (NSC-AD; AG09088.1) and the NSC Huntington's disease line (NSC-HD1; GM02191.1), were used to perform the assay. The cells' identity was confirmed through positive staining for NSCs markers. All the cell populations tested presented uniform expression of the listed markers, indicating successful induction to neural stem cell state (Figure 3).

NSCs are a progenitor cell type capable of differentiation into neuronal cells, which are the cell types of interest for our studies. Thus, we tested the ability of the previously generated NSCs lines to successfully differentiate into neurons. To do this, wild type NSCs were plated and cultured in complete StemPro® NSC Serum Free medium until reaching 80% confluency. Differentiation was then initiated by switching to general neuronal differentiation media, partly (1/2) replenished daily. Three slightly different differentiation media were tested to determine their relative efficiency. Cells were cultured in either complete B27 medium, complete B27 medium supplemented with 500 nM of purmorphamine, or complete B27 medium supplemented with 500 nM of purmorphamine and 50 nM of retinoic acid. Complete B27 medium was chosen as it is the most commonly adopted serum-free medium for neuronal culture [40]. The supplement purmorphamine was chosen for its ability to induce the initiation of neuronal differentiation [41], and retinoic acid was chosen as it inhibits neural cell proliferation while promoting their differentiation [42]. We tested each combination to determine if the addition of each of the supplements would have a significant impact in promoting the differentiation of NSCs to neurons, and in the ability of maturing neurons to grow rapidly and efficiently. At Day 14 of differentiation,

immunocytochemistry staining was performed targeting the neuronal marker MAP2, and all the cell populations presented its uniform expression, indicating that the protocols adopted induced neuronal differentiation (Figure 4). The relative expression of MAP2 was associated to the size of the axonal outgrowths formed in each of the cultures tested. To determine efficiency of neuronal differentiation protocols, we quantified primary neuronal outgrowth using NeuronJ in ImageJ software. Briefly, 8-bit images of MAP2 positive cells were used to determine pixel length of neurite outgrowth from cell bodies. The highest values for the average length of primary axonal outgrowths (in pixels) were observed for the cells cultured in B27 medium supplemented with 500 nM of purmorphamine and 50 nM of retinoic acid (Figure 4). Therefore, this protocol was deemed the most efficient and was adopted in successive neuronal differentiations.

Neuronal identity was confirmed through immunocytochemistry staining of 14-day old neurons generated starting from the cell lines NSC-AD, NSC-wt, and NSC-HD1. The assay targeted NSC markers and neuronal markers. Uniform expression of the neuronal markers (Figure 5), as well as suppression of the NSC markers (result not shown) confirmed the successful differentiation of NSCs into neurons in all the cell lines. Neurons can be classified according to the neurotransmitter that they produce and adopt to transmit signals within the organism. They can be distinguished as cholinergic neurons, producing acetylcholine; GABAergic neurons, producing gamma aminobutyric acid; glutamatergic neurons, producing glutamate; dopaminergic neurons, producing dopamine; and, finally, serotonergic neurons, producing serotonin. The neuronal differentiation protocol that we adopted induced a general neuronal differentiation, without directing differentiation to any specific neuronal type. I therefore attempted to perform a preliminary characterization of the neuronal populations generated by targeting GABAergic and adrenergic markers, and establish if these two types of neurons were produced. Positive staining

for the GABAergic markers (Figure 5), and negative staining for the adrenergic marker (result not shown), indicated that the general neuronal differentiation protocol adopted favored the formation of GABAergic neurons over adrenergic ones. Altogether, these data indicated that all of our NSCs lines were capable of differentiation into neurons, and that the general protocol adopted enabled the generation of GABAergic neurons.

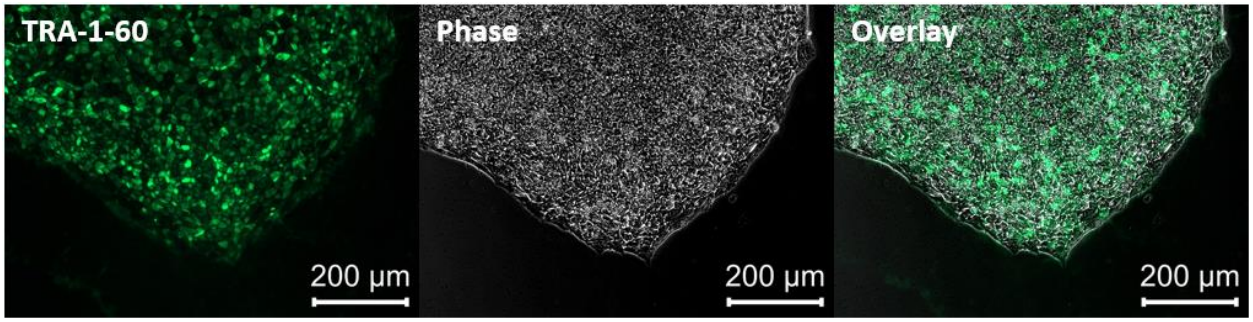

Figure 1. Live staining of an induced pluripotent stem cell colony. Positive staining for TRA-1-60 confirms the pluripotency of the colony. Coincidence of the pluripotent region with the phase image of the colony indicates the absence of differentiated regions, and suitability of the colony to be expanded or adopted for the neural induction protocol.

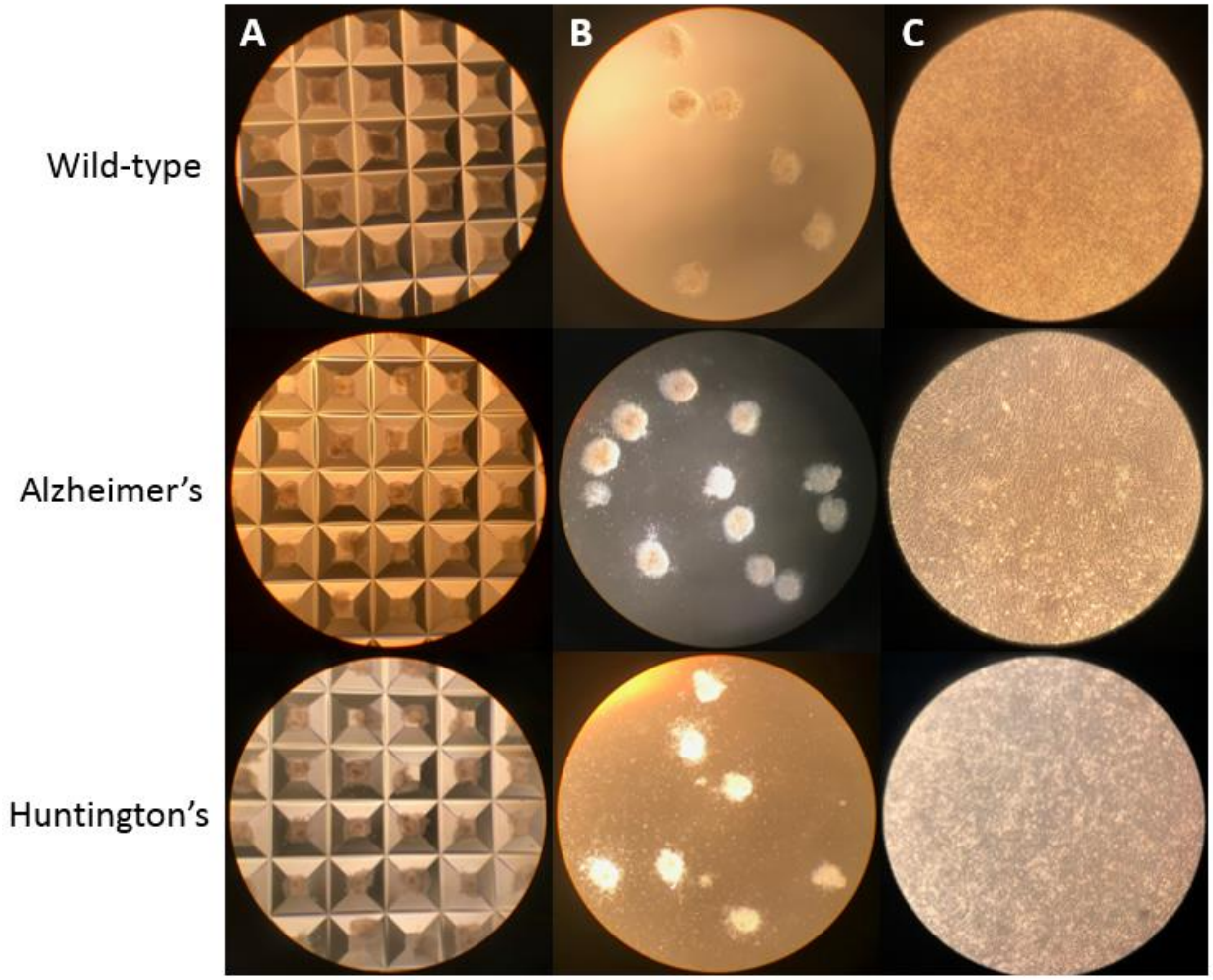

Figure 2. Neural induction protocol progression. The wild-type (bASC3.2), Alzheimer's disease (AG09088.1), and Huntington's disease (GM02191.1) cell lines were adopted for the purpose. Depicted are the cells at the embryoid body stage in an Aggrewell™ 800 plate (A), the embryoid bodies replated on Geltrex® (B), and neural stem cells (C).

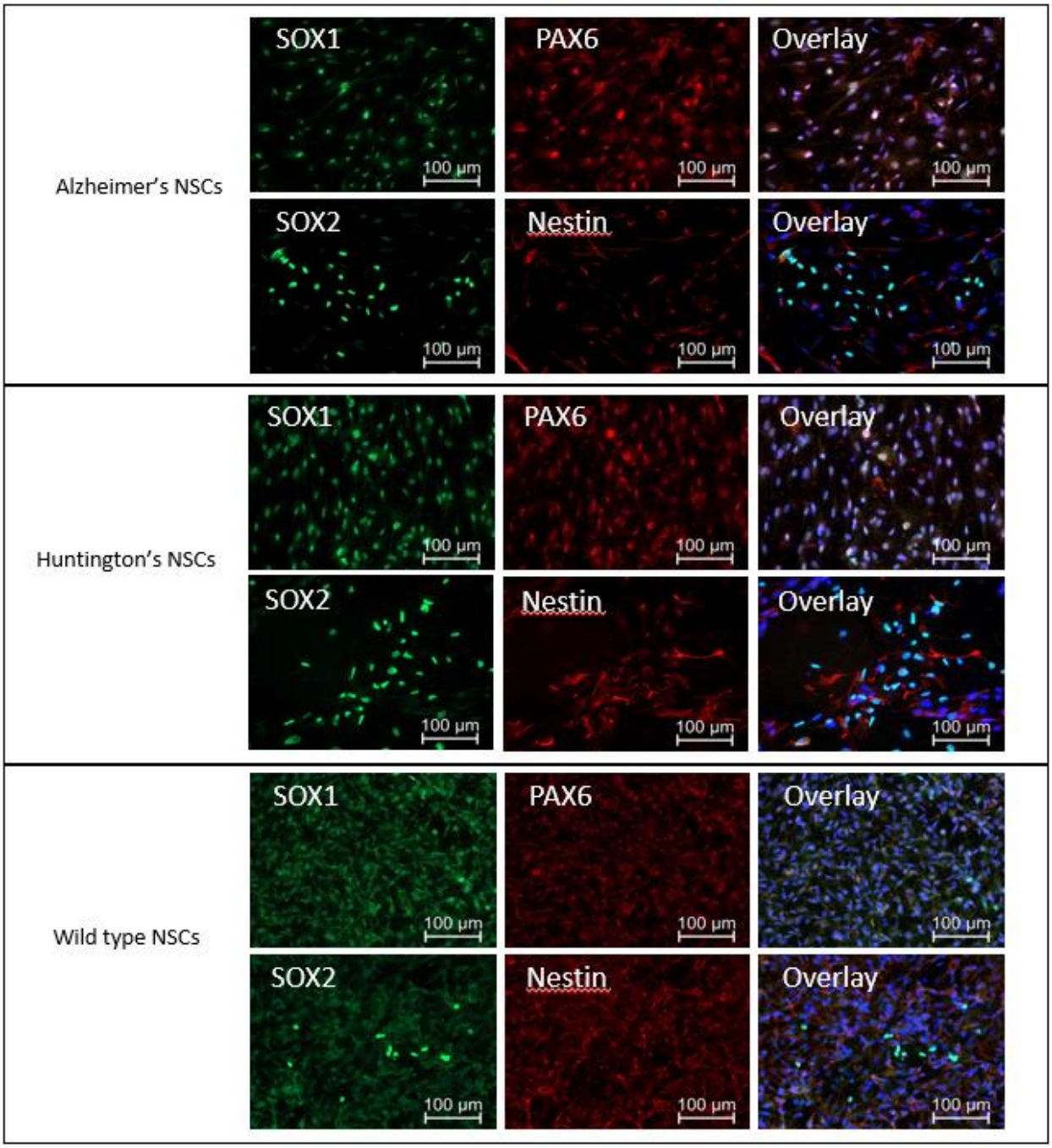

Figure 3. Efficiency of the neural induction protocol was determined performing immunocytochemistry assays on NSCs populations. Cells of the lines NSC-AD, NSC-HD1, and NSC-wt were tested, and presented uniform expression of multipotency and NSCs markers SOX1, SOX2, PAX6, and Nestin. All cultures were counterstained with DAPI. Size standards 100 µm.

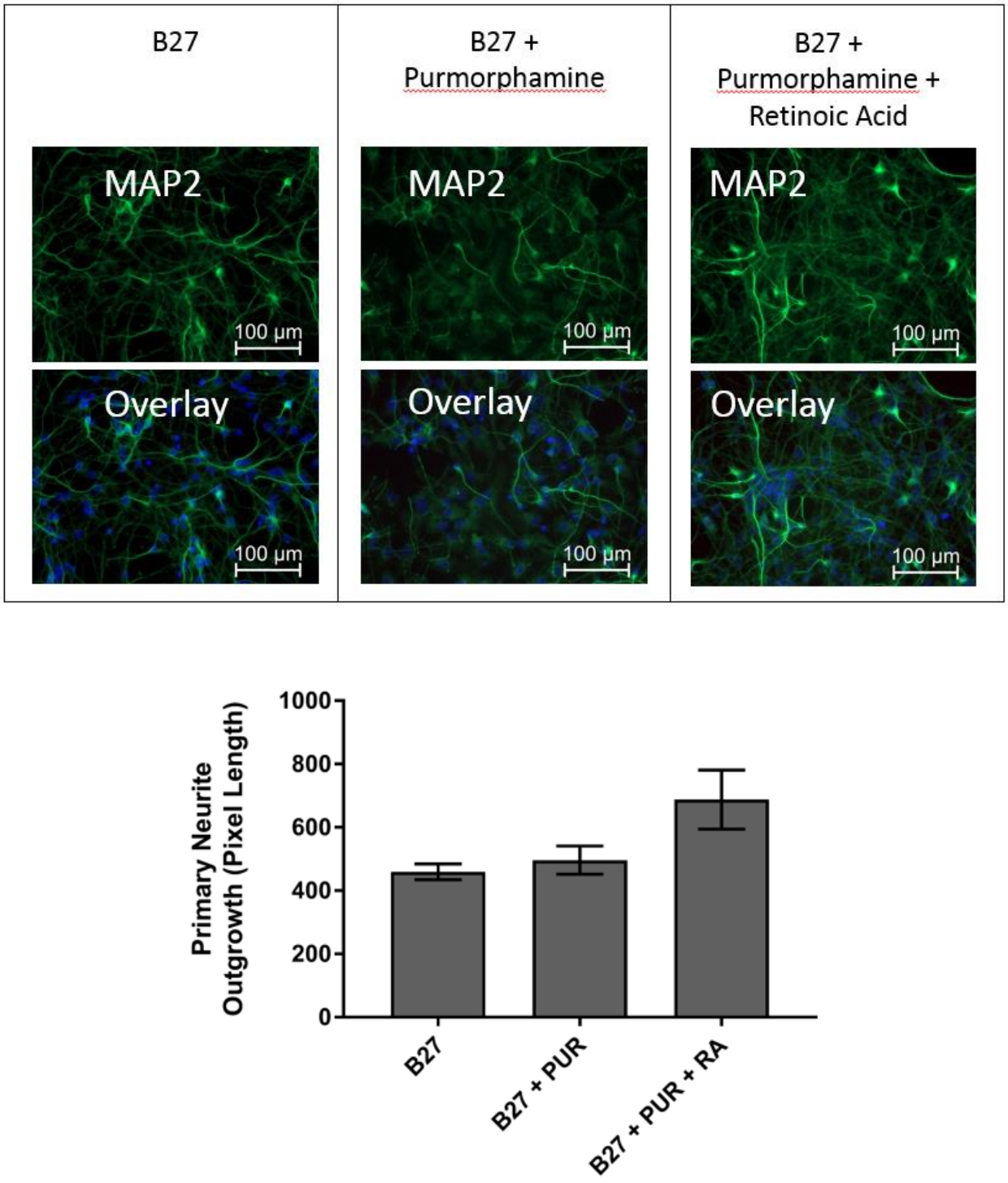

Figure 4. Selection of a neuronal differentiation protocol based on their relative efficiency. Neuronal differentiation was performed on 80% confluent NSCs using B27 medium, B27 medium supplemented with 500 nM of purmorphamine, or B27 medium supplemented with 500 nM of

purmorphamine and 50 nM of retinoic acid. In the figure, green indicated expression of MAP2 marker, blue indicated expression of DAPI nuclear stain, and the size standards were 100 µm. Following quantification of average length (in pixels) of primary axonal outgrowths using the NeuronJ in ImageJ software, B27 medium supplemented with 500 nM of purmorphamine and 50 nM of retinoic acid was deemed the most efficient protocol.

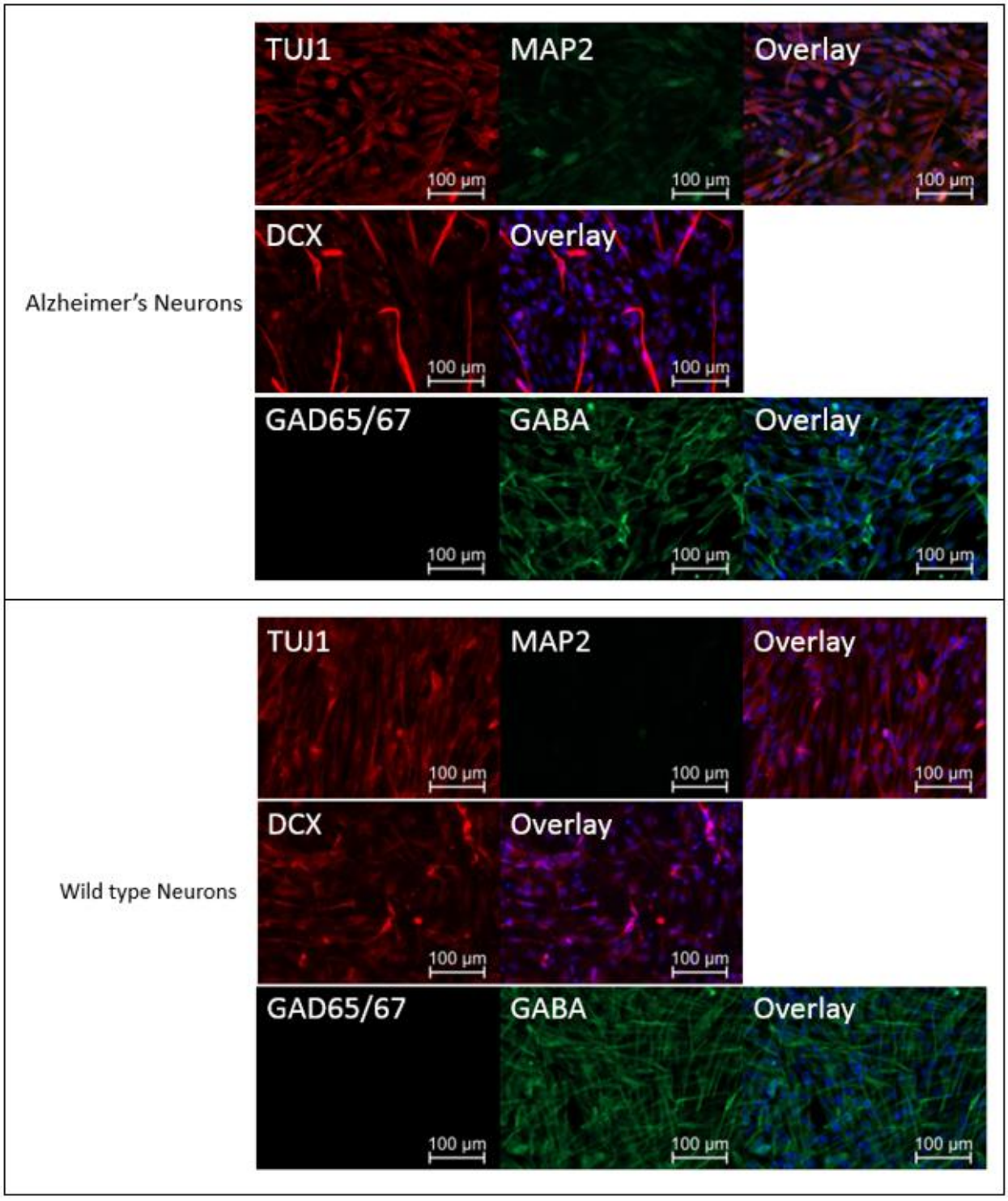
Alzheimer's Neurons
TUJ1
MAP2
Overlay
DCX
Overlay
GAD65/67
GABA
Overlay
Wild type Neurons
TUJ1
MAP2
Overlay
DCX
Overlay
GAD65/67
GABA
Overlay
100 µm

Figure 5.

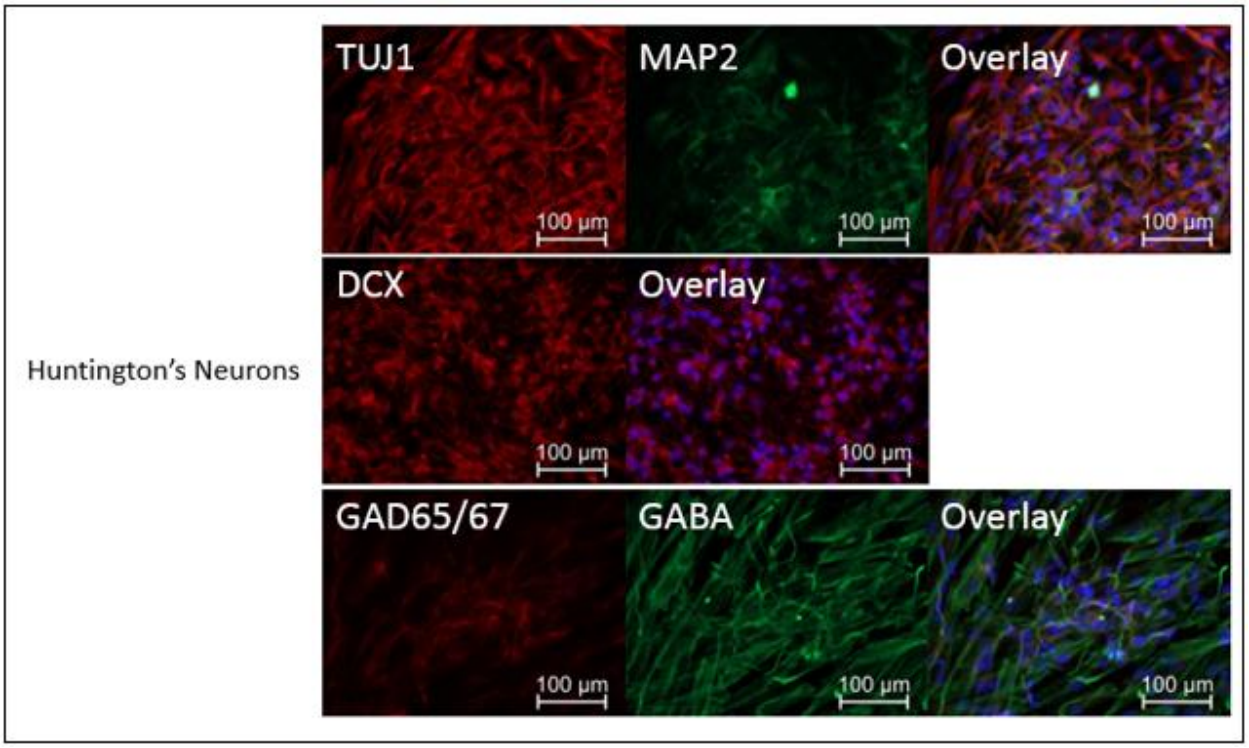

Figure 5 cont. Efficiency of the neuronal differentiation protocol was evaluated through immunocytochemistry staining of 14-Days old neurons obtained from differentiation of the cell lines NSC-AD, NSC-wt, and NSC-HD1. Expression of the neuronal markers TUJ1, MAP2, and DCX confirmed the successful differentiation into neurons. Additionally, expression of the GAD65/67 and GABA markers indicated differentiation into GABAergic neurons. All cultures were counterstained with DAPI nuclear stain. The size standard was 100 µm.

MEAs cell culture and recording

After generation of the cell lines NSC-wt, NSC-HD1, NSC-AD, and their successful differentiation into neurons, I proceeded to apply an MEA system for the study of their electrophysiological properties. Cells of the neural lineage are known to produce spontaneous activity in the form of transmembrane voltage fluctuations, and I tested the system and compared the spontaneous electrical activity of NSCs and maturing neurons. This portion of the last aim was fundamental to establish the most appropriate protocols for the use of MEA systems to study the spontaneous activity of neural networks, and their suitability to become part of a more sophisticated three-dimensional cell culture system.

Electrophysiological studies with MEAs systems were conducted with the goal of establishing the presence of spontaneous activity of NSCs and neuronal networks of wild type and disease cells [24, 43]. The cell lines NSC-wt and NSC-HD1 were adopted to perform this experiment. MEA plates were coated with Geltrex® matrix and NSCs were enzymatically passed from a 100% confluent well of a 6-well plate to 6-8 MEA plates (Figure 6). When the NSCs reached 80-100% confluency on selected MEA plates, neuronal differentiation was initiated. A second coating protocol was adopted to determine if the use of a different substrate for cell culture would result in altered quality of the electrophysiological readings. Therefore, the MEA plates were alternatively coated with laminin, and seeded with NSCs or maturing neurons previously differentiated on Geltrex®-coated plates.

To establish the presence of spontaneous activity, measurements of electrical activity of neural stem cells and neurons were taken for five-minute intervals. Data produced by primary rat cortical and spinal cord neuron populations, and measured at the Neural Engineering Lab for scopes outside of this project, were used as positive control. The recording software MC_Rack

V4.5.10 allowed real-time visualization of the electrical activity measured at each recording electrode in the form of graphs presenting the change in voltage over time. Voltage changes above the set 5-standard deviation threshold were attributed to cell activity, and distinct waveforms could be observed with regard to the voltage-change pattern associated with each spike. Signals recorded from neural stem cells populations (plated either on Geltrex® or laminin) presented significant noise, and no spikes attributable to spontaneous cell activity were observed. Spike-like activity was present, but the waveforms generated were credited to artifact signals due to environmental disturbances. Spikes were identified as artifacts following visual analysis of the real-time recordings, based on their characteristic shape and the fact that they were simultaneously generated on various electrodes on the MEA plates. No differences were observed in the type of signals produced by NSC-wt or NSC-HD1 cells. Data collected from maturing neurons also presented high noise ratios, and no significant spikes were observed for wild type or Huntington's disease cells plated and differentiated on Geltrex®. Differently, scarce but relevant spikes were recorded from neurons plated on laminin.

The MC_Rack V4.5.10 software allowed for analysis of the raw data recorded, which was constituted by the voltage values at each measuring time point. Spikes within the recording interval were individuated when the amplitude of the measured voltage exceeded the set threshold. The time points corresponding to each spike were used to generate raster plots representative of the neural network's activity (Figure 7). These graphs are a schematic representation of all the electrodes in the MEA plate versus the recording time. Each spike measured is visualized in the graph as a darkened region in correspondence of the recording electrode and the relative time at which the spike was observed. Raster plots provide an accessible way to analyze the activity of a neural network, showing the activity of the few cells in contact with each electrode, as well as

emphasizing the overall activity of the cell network and highlighting potential synchronization episodes. We generated a raster plot with the firing activity of neurons differentiated from NSC-wt and plated on a laminin-coated MEA, and we compared our plot to a typical raster plot obtained from rat primary spinal cord neurons recordings. The levels of activity observed in the maturing neurons were significantly reduced compared to the positive control, and no firing pattern was observed. Optimization of the plating protocol adopted will be necessary for improved results.

The waveform corresponding to the voltage change generated by the transmission of signals, is a distinct characteristic of each neuron. Analysis of the raw data allows for the extraction of the specific waveforms of each spike, and isolation of waveforms significantly different in shape can be attributed to the fact that they were generated by different cells. Electrodes on the MEA plates can record signals generated by multiple cells in contact with them. Analysis of the raw data produced by each channel using software such as MATLAB is an effective tool to determine the number of cells on each electrode. Starting from the control raw data obtained from rat primary spinal cord neurons, I generated a MATLAB code able to individuate spikes present in 30-second intervals, after setting a threshold of 0.01 V, and extract the waveforms of each spike. Superimposing and comparing the extracted waveforms allowed me to determine the number of distinct shapes present, and consequently the number of firing cells in contact with the recording electrode in analysis, which in this case was only one (Figure #). The same code has the potential to be applied to raw data recorded from the neural cells that we previously generated. However, due to the absence of significant spiking activity in any of the recording electrodes on the MEA plates, it was not possible to analyze the raw data and extract waveforms prior to further optimization of the coating and seeding protocol.

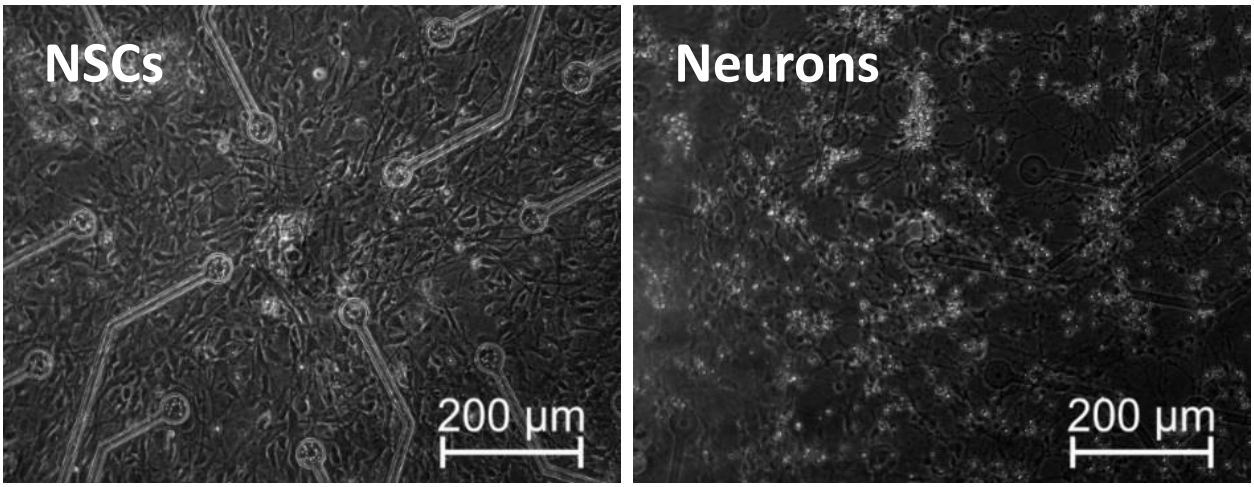

Figure 6. Wild type NSCs on Geltrex®-coated MEA plates two days after plating; Wild type maturing neurons at Day 11 of differentiation on Geltrex®-coated MEA plates. Increased cell death, compared to NSCs, and prominent axonal outgrowth are observed.

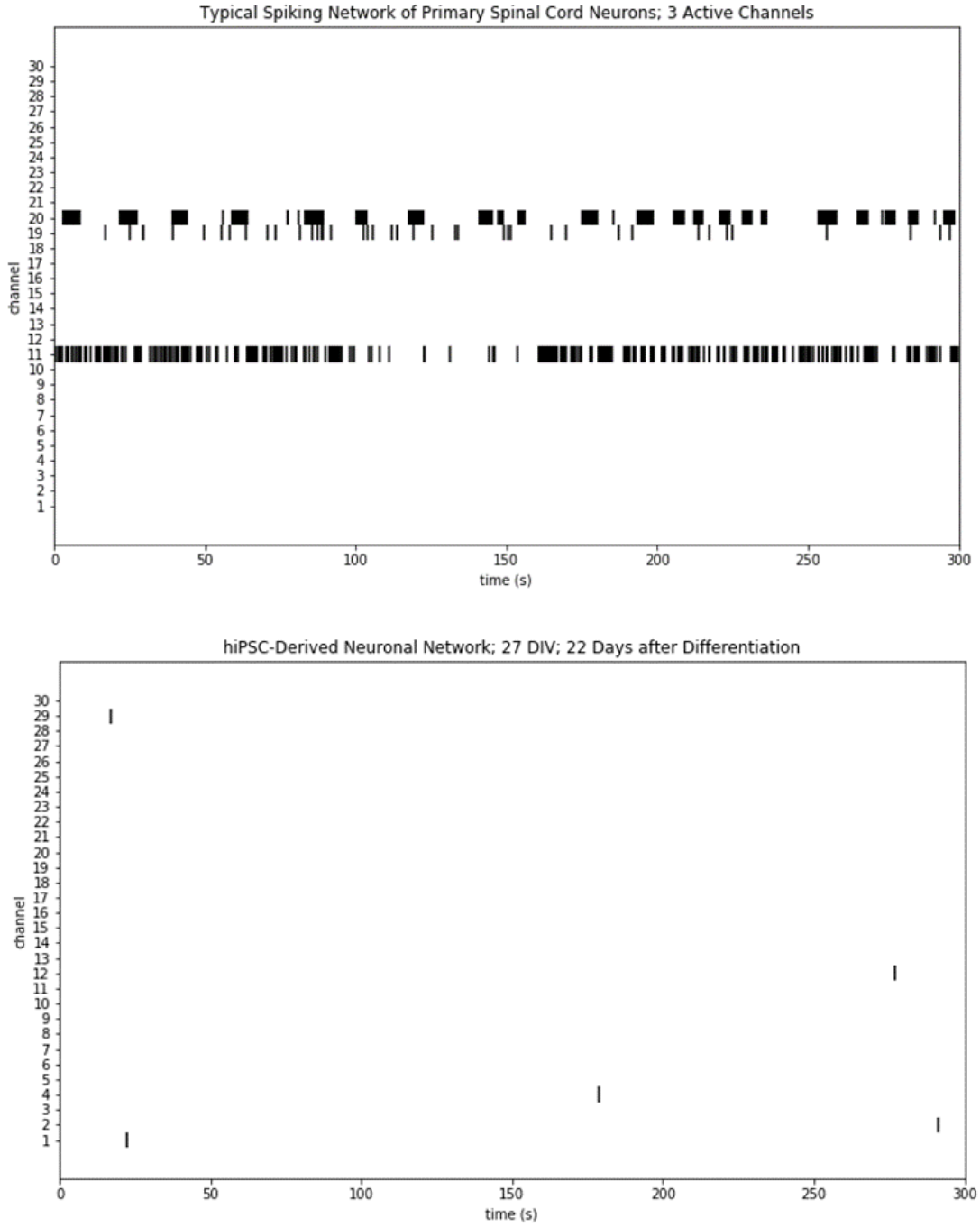

Figure 7. Example of a typical raster plot generated by rat primary spinal cord neurons (top). Only three of the thirty recording electrodes in the MEA plate were clearly active, and spikes were reported at a high frequency throughout the 300-second recording interval. Differences in the spiking pattern between the three electrodes can be attributed to the specificity of each neuron's

electrophysiological characteristics. Raster plot generated with data obtained from maturing neurons plated on laminin-coated MEA plates (bottom). Significantly reduced activity was observed, compared to the positive control.

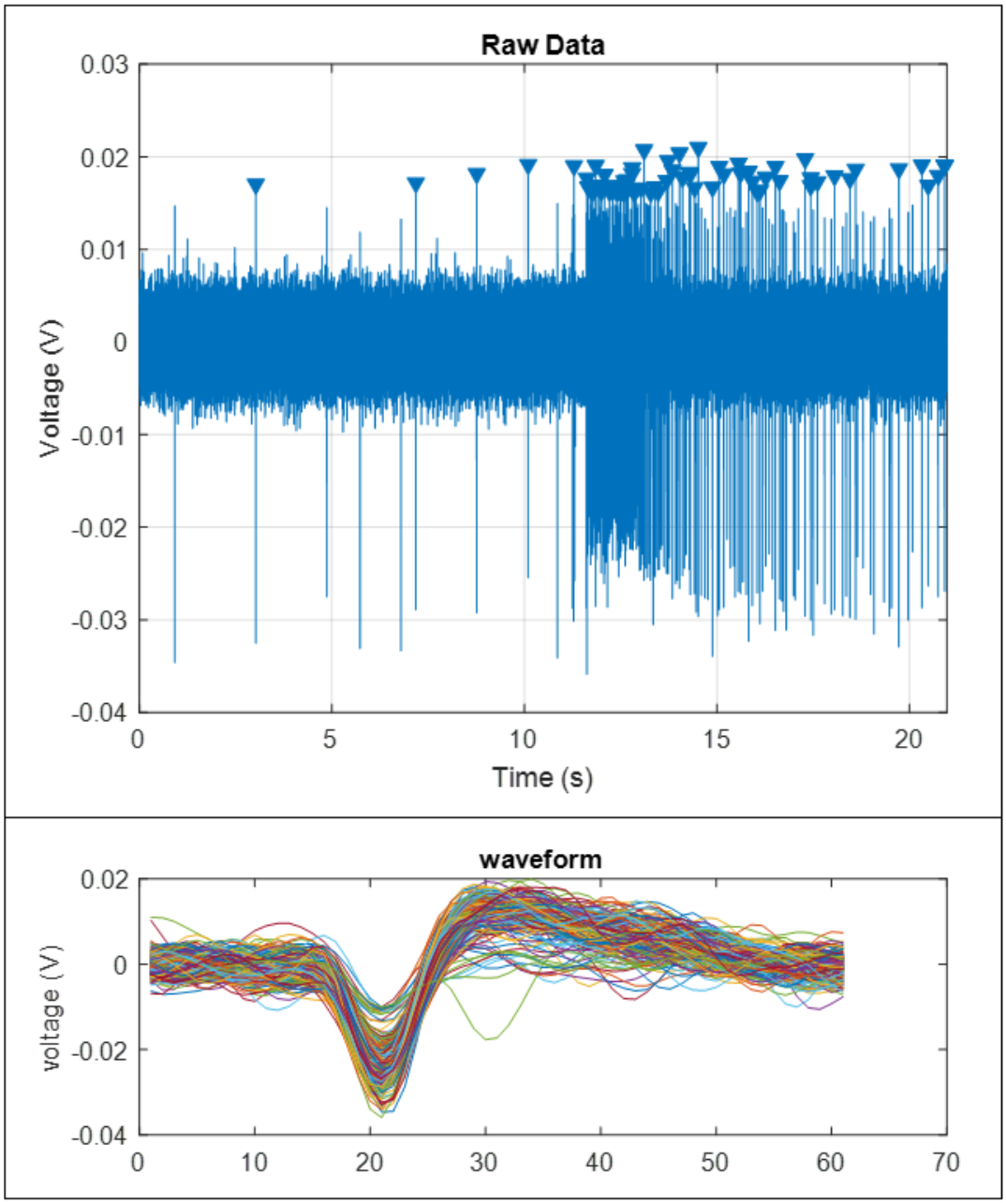

Figure 8. Raw data obtained from rat primary spinal cord neurons. Spikes were individuated and labeled after arbitrarily setting a voltage amplitude threshold of 0.01 V. Waveforms of each spike were extracted and superimposed. Their uniform shape indicates that all the spikes were produced by a single firing cell on the recording electrode.

b. Aim (2) – Fabrication of porcine brain matrix-derived hydrogels suitable for cell culture

In the second portion of this project, I aimed at developing a porcine brain extracellular matrix-derived substrate, suitable for culture of iPSCs and neural lineage cells. This tissue based ECM should contain all of the necessary signaling and structural elements to elicit biomimetic responses from neuronal cells.

Successful fabrication of porcine-brain derived hydrogels

The first step in the protocol for the formation of ECM derived hydrogel consisted in the retrieval of animal brain tissues. Whole porcine brains were successfully extracted and all the structures of the cerebrum, cerebellum, midbrain, pons, medulla, and part of the optic nerves and spinal cord were preserved (Figure 8A). The meninges layers and the blood vessels embedded in the brain tissue were removed as best as possible before proceeding with the protocol implementation. Complete decellularization of the brain was then performed over a 4 – 7 days' period (Figure 8B), depending if the brains were cut into smaller sections prior to decellularization or they were left whole. Decellularization solution was completely replenished every 24 hours, and it was observed that complete discard of the supernatant results in poor final product yields. This can be attributed to the characteristic low content of fibrous or basement ECM proteins in the brain, and high proteoglycan contents [44]. Proteoglycans interact with several components, including soluble factors, and are more easily dissolved in the decellularization solvent [45]. To overcome excessive loss of product, the supernatant was spun in a high-speed centrifuge at 17,500 x g for five minutes, allowing recovery of the dissolved ECM protein and discard of the decellularization solution. Product was washed once in IPA, lyophilized (Figure 8C), and digested in 1 mg/ml solution of pepsin from porcine gastric mucosa in 0.1 M HCl (Figure 8D). Digestion

was performed for 24-72 hours, until formation of a visibly viscous solution, and the product was filtered through a 40 µm strainer. Larger pieces of undigested ECM were re-diluted in pepsin solution and underwent prolonged digestion. The filtered product was dialyzed against PBS to bring the product to neutral pH, and aliquots were preserved at -80℃ until ready to be used for hydrogel formation.

The ultimate goal of this experiment was the generation of ECM-derived hydrogels, onto which cells can be injected and cultured. The ability of the product to spontaneously gel at elevated temperatures was tested plating diluted product on plastic cultureware and incubating overnight at 37℃. Serial dilutions from 100% to 5% of the brain-derived matrix in DMEM/F-12 were prepared, and successful gelling was observed at matrix concentrations superior to 30% (Figure 8E).

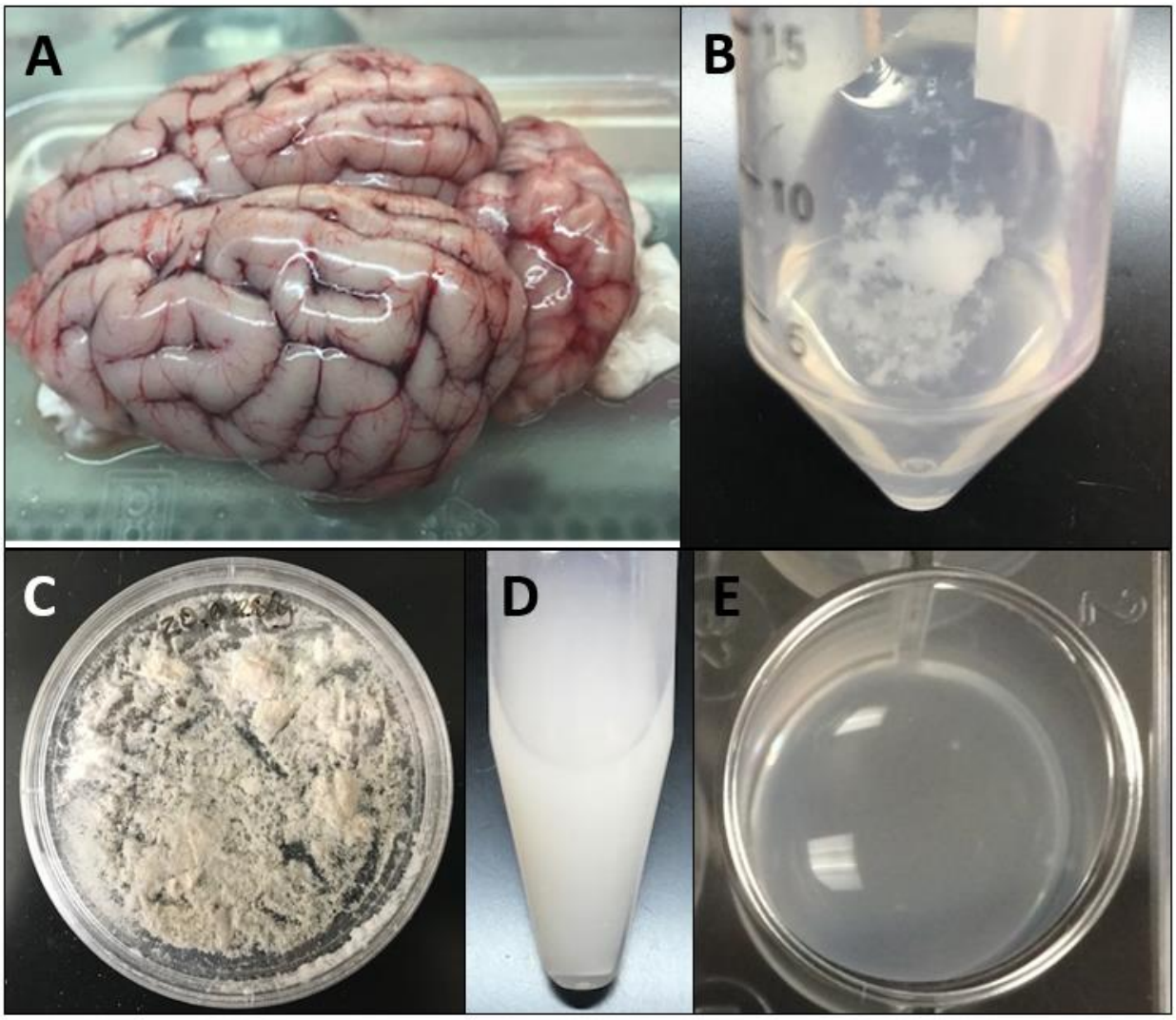

Figure 9. Steps in the fabrication of the brain-derived matrix product. (A) Whole brain extracted from porcine head. In the figure, the Dura Mater was removed, while the Arachnoid and Pia Mater and the embedded blood vessels are depicted. (B) Decellularized brain tissue. (C) Lyophilized product obtained from the processing of a whole porcine brain. (D) Pepsin digestion process. (E) Hydrogel spontaneously formed after incubation of the final product at 37℃.

Formation of tissue-specific substrates that more closely mimic the natural cellular environment contributes to the formation of highly biomimetic cell culture systems. The minimal presence of nucleic acids embedded in the substrate is fundamental for the ability of cultured cells to survive and proliferate in such an environment. I therefore evaluated the efficiency of the decellularization protocol first through Hematoxylin and Eosin staining of paraffin embedded sections (Figure 9). Samples from different anatomical regions were collected to observe the variability in cellular content of different areas of the porcine brain, and were used as positive controls. In non-decellularized samples collected from cerebrum, cerebellum, medulla, pons, and midbrain, eosin-stained nuclei were clearly visible as well as the hematoxylin-stained proteins. The decellularized product presented no nucleic acid-staining, while the protein staining was preserved. This indicated efficiency of the protocol in removal of cells and preservation of extracellular proteins. To further confirm the protocol's efficiency, gDNA content of native and decellularized tissue was measured. The decellularized tissue presented a gDNA content reduced by about 65% compared to the positive control.

The protein composition of tissue's extracellular environment plays a role in the definition of the physical and biochemical characteristics of each tissue [46]. Definition of the ECM protein components of the brain-derived product were conducted to determine its similarity to commercially available products and establish its suitability for cell culture purposes. The protein content of the final product was quantified through DC^{TM} assay and compared to a serum albumin protein standard. The final total protein concentration of the brain-derived hydrogels was measured as 6.4 mg/ml. The protein composition of the brain-derived hydrogel was qualitatively analyzed via PAGE assay (Figure 10). The product was run on a polyacrylamide gel, and compared to Geltrex® matrix and a ladder positive control. The assay showed that the main protein components

of the brain-derived product and those of the commercially available matrix are comparable. Geltrex® has been extensively characterized, and its main protein components are laminin, collagen IV and entactin. It is therefore possible to attribute the three major bands obtained performing PAGE assay of the Geltrex® matrix, and observed between 200-300 kDa, and 100-130 kDa, to such proteins. Multiple bands were also observed performing the assay respectively to the brain-derived matrix and confirming the preservation of intact proteins following the hydrogel-formation protocol. Bands were observed both in correspondence of those characteristic of Geltrex® and in additional locations that indicate smaller protein size. From this result it is possible to infer that the major protein components of the brain-derived product are laminin, collagen IV, and entactin, and that the product is also rich in smaller and yet unidentified proteins.

The ultimate goal of this experiment was to produce a substrate suitable for three-dimensional stem and neural cell culture. This includes the coating of cultureware to maintain monolayer cultures, and injection of cells within the substrate to allow them to grow three-dimensionally. The suitability of the product for neural cell culture was therefore tested coating cultureware with the brain-derived product diluted in DMEM/F12, and through in vivo injections in rat models. NSC-wt cells were seeded on the coated plates and incubated at 37℃. Cells on multiple plates were not able to stick to the plates' surface, and instead they adhered to each other forming cell clumps floating in the media (result not shown). However, the brain-derived matrix injected in vivo allowed for survival of the iPSCs and NSCs over the ten-week period, demonstrating the biocompatibility of the product. This was in contrast to iPSCs and NSCs injected in the rat's mammary tissue in absence of the brain-derived matrix, which did not survive in any of the samples (Figure 11). The potency of the cells was confirmed through immunohistochemistry staining of paraffin-embedded samples (Figure 12). Expression of the

SOX2 marker was observed in both iPSCs and NSCs injected in brain-derived hydrogels in rat models, confirming that both cell lines conserved their potency during the incubation period.

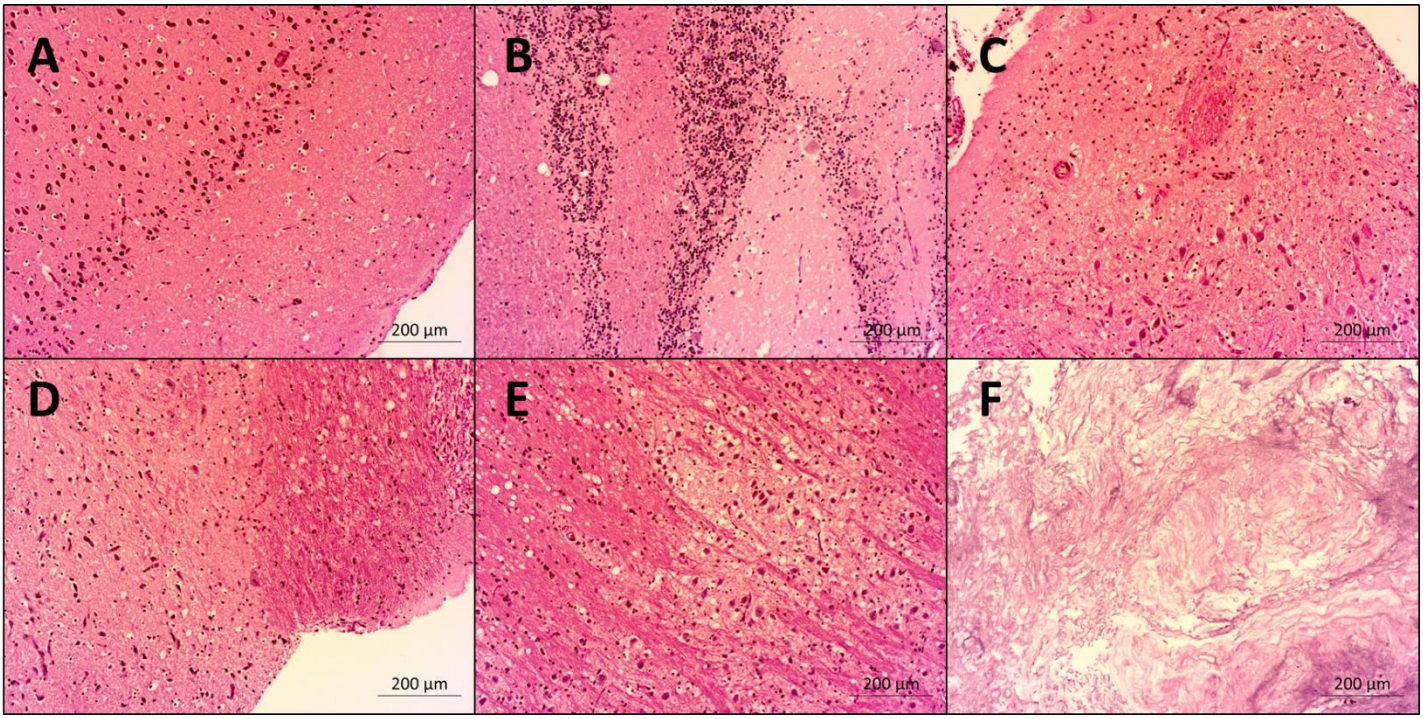

Figure 10. Hematoxylin and Eosin staining was performed on paraffin embedded samples retrieved prior and following the decellularization process. In untreated samples from, respectively, cerebrum, cerebellum, pons, medulla, and midbrain (A-E), the presence of nuclei and extracellular proteins is clearly shown by positive staining for both hematoxylin and eosin. In decellularized tissue (F), negative staining for hematoxylin and positive staining for eosin demonstrate the absence of cells in the sample, and confirm the efficiency of the adopted protocol. Size standard 200 µm.

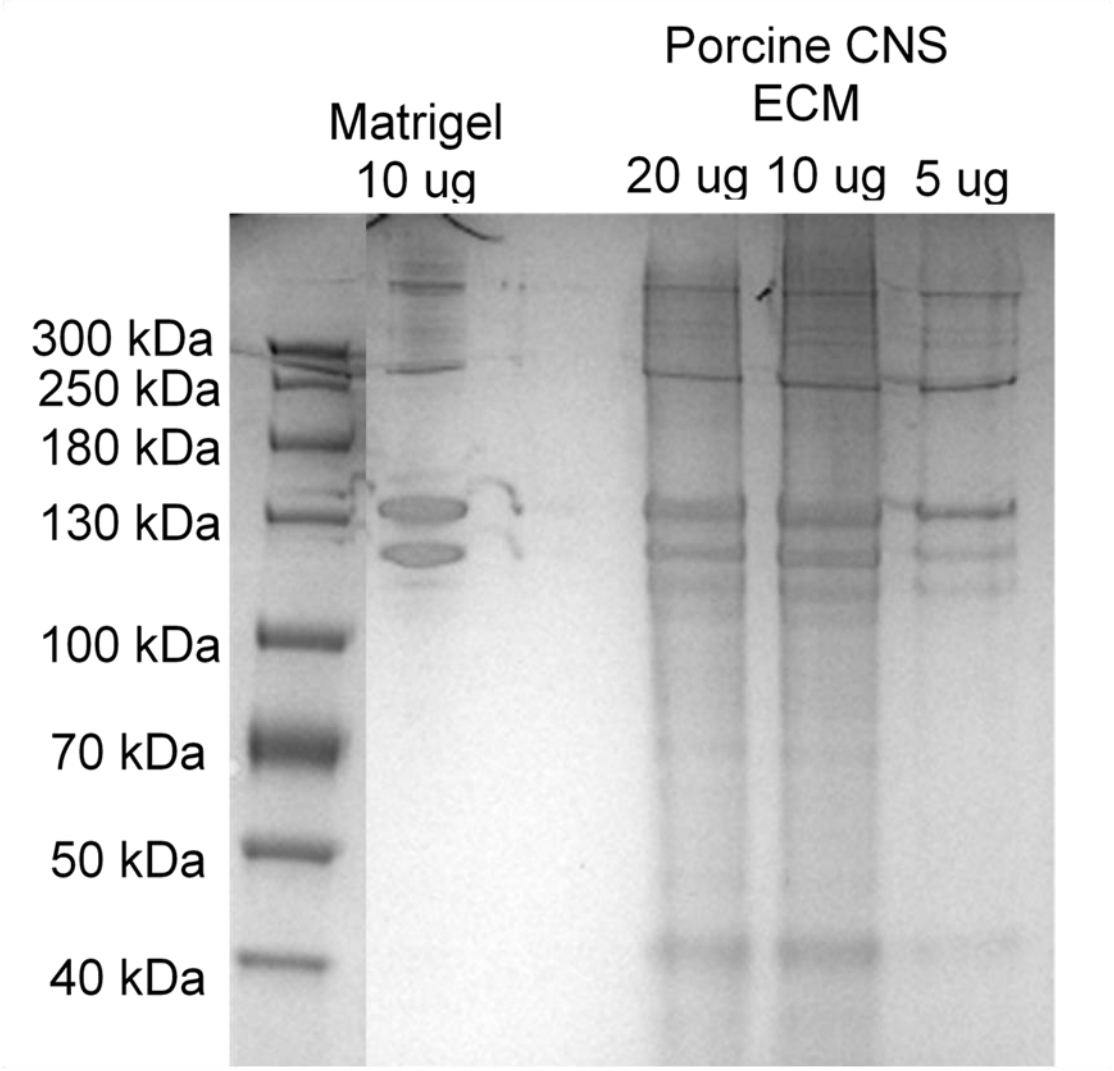

Figure 11. PAGE assay was performed to qualitatively analyze the protein content of the brain-derived product. The major bands, observed between 200-300 kDa, and 100-130 kDa were present in both Geltrex® and porcine brain matrix. These can be attributed to Geltrex®'s main protein components laminin, collagen IV and entactin. Additional bands indicating the presence of lower-weights proteins are observed.

Figure 12. The biocompatibility of the porcine brain-derived product was tested injecting NSCs in rats' mammary tissue. In absence of brain-derived matrix, no change in the morphology of the tissue was observed after injection of NSCs and incubation in any of the samples (A). When the NSCs were injected in porcine brain matrix placed within the mammary pad, observable growths were present in the samples following incubation (B).

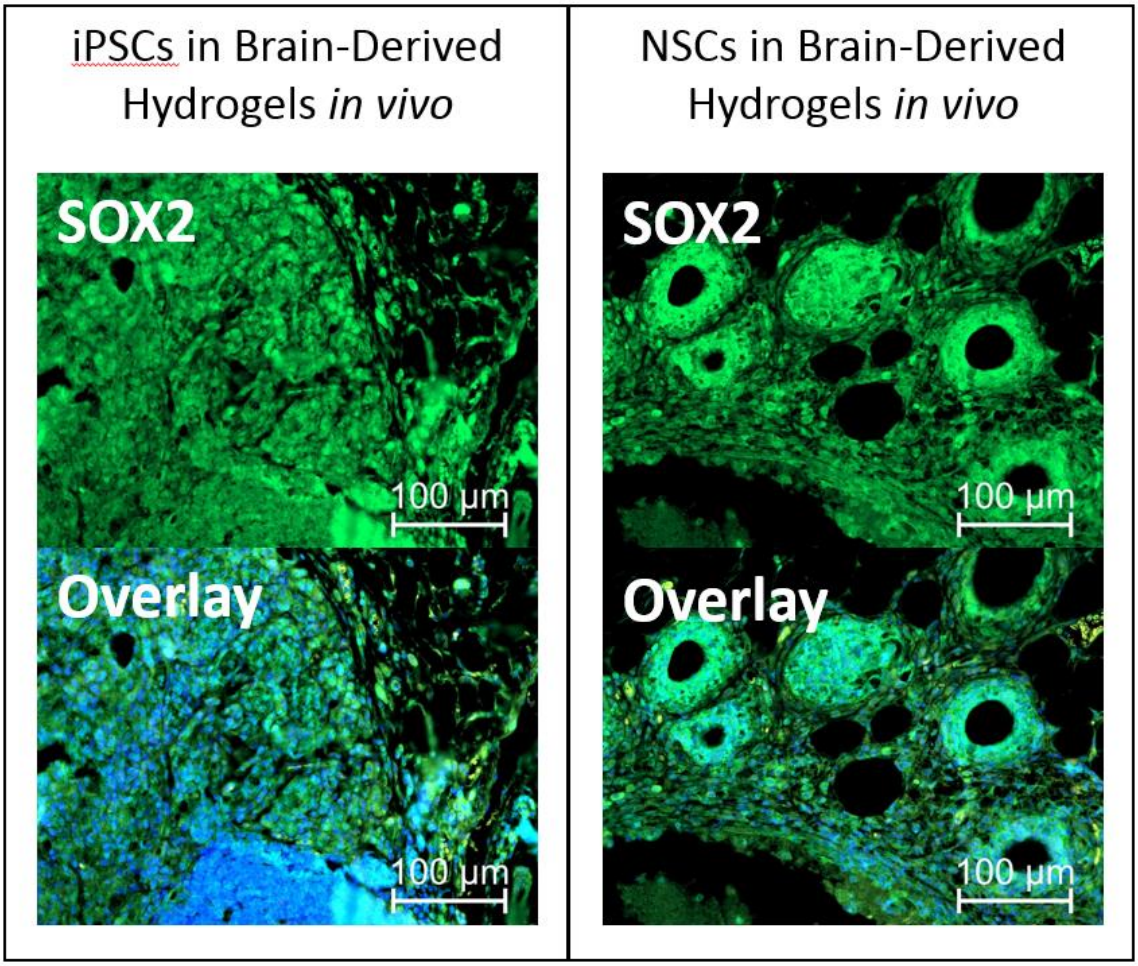

Figure 13. Immunocytochemistry assay of iPSCs and NSCs injected in brain-derived hydrogels in rat models. Expression of SOX2 in NSCs and iPSCs after incubation confirmed the preservation of the cells' potency, indicative of the ability of the hydrogels to promote cell survival and proliferation. All cultures were counterstained with DAPI nuclear stain. Size standard was 100 µm.

Aim (3) – Optimization of a 3D extrusion-based bioprinter to obtain single cell/single beads resolution printing.

The last portion of the project aimed at the optimization of the parameters of a 3D extrusion-based bioprinter to perform single-cell/single-beads resolution printing. The ultimate application of such systems entails the printing of single NSCs and WNT transcription factors conjugated to fluorescent beads into various substrates. By achieving the critical single cell separation of NSCs in a high-throughput array we would be able to study of the mechanisms of NSCs asymmetrical division at a single cell resolution.

3D Extrusion-Based Bioprinting System

A 3D extrusion-based bioprinter represents the ideal instrument to perform injections of a selected number of cells into specified 3D locations and ultimately enable the study of NSCs asymmetrical division at a single cell resolution. The system used was adapted from the commercially available model Felix 3000 (Figure 13A). Prints were performed on either 24 well plates or PEN membrane slides placed on the printer's moving bed. The aim of this experiment was the achievement of single-cell/single-beads resolution printing, to enable the study of asymmetrical division in the context of single cells. This would be achieved printing NSCs conjugated to Fluorospheres®-labeled WNT beads, and studying the ability of NSCs to divide asymmetrically and differentiate, relatively to their contact to the WNT transcription factor. To achieve single-cell/single-bead resolution printing needles of about 100 µm in diameter (measure relative to the inner diameter of the needle's opening) were fabricated (Figure 13B). Smaller tip inner diameters were found to prevent cells from being easily delivered during the extrusion

process, while the use of significantly larger diameters resulted in the delivery of an excessive number of cells during each single print.

Starting from a cell concentration of 300,000 RFP-MCF12A/ml, the extrusion value most suitable to achieve single-cell printing was determined experimentally (Figure 14). The extrusion value parameter refers to the amount of fluid (in this case cell solution) injected into the substrate for each print, and corresponds to the travel of the lead screw in mm to achieve such injection volume. It is calculated accounting for the diameter of the needle and cell concentration, as well as the desired cell density of the print. MCF12As or MCF7s (both human breast derived cell lines) were chosen to evaluate the single cell performance of our printer as they are easy to culture, and they are constitutively fluorescently labeled with either GFP or RFP, thus are easy to visualize. Cells were resuspended in 0.005 M EDTA in PBS and injected into 1% agarose gels. Starting from an extrusion value of E=0.001 to one of E=0.017, ten prints were performed for each value to determine which produced the most consistent number of single-cell prints. Upon visual analysis on a Zeiss Axio microscope at 20X magnification, it was concluded that an extrusion value E=0.009 was the most suitable to achieve single-cell resolution printing. Printing was repeated with the chosen extrusion value, and following DAPI nuclear staining the printing resolution was determined to be 35%, relatively to single cells (Figure 15).

Printing with the same parameters was then performed with the addition of Red FluoSpheres® Fluorescent Microspheres. Printing was optimized using Corning® Collagen I, High Concentration, Rat Tail hydrogels, aiming to achieve single-cell/single-bead resolution printing. Following visual inspection of images acquired with a Zeiss Axio microscope at 20X magnification, the printing resolution achieved was determined to be 13%, relative to successful single-cell/single-beads prints. An average of 2 cells per injection, with standard deviation 1.3 was

achieved, while beads were printed with an average of 0.76 per injection with standard deviation 0.78 (Figure 16).

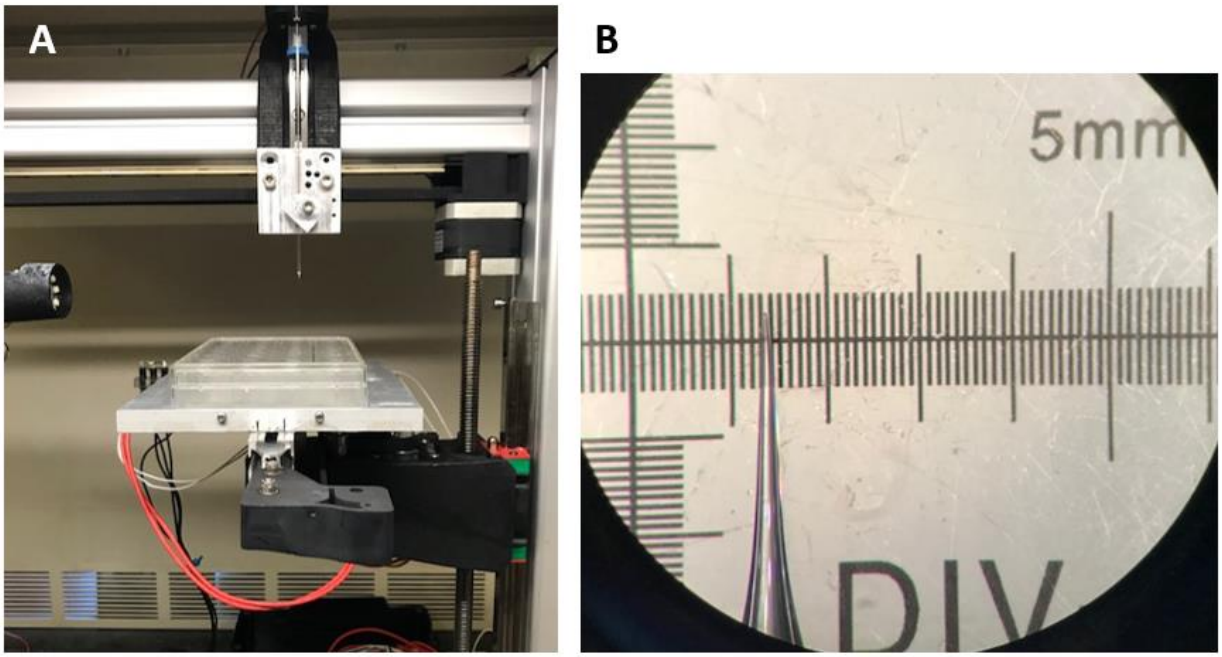

Figure 14. (A) 3D extrusion-based bioprinter setup. In the field of view are included the moving bed and the cultureware inserted at the moment of printing. The needle placement to perform the injections is also shown. (B) Needle size was adjusted to 100-500 µm in inner diameter to prevent 4cell clogging at the tip while allowing passage of at least a single cell.

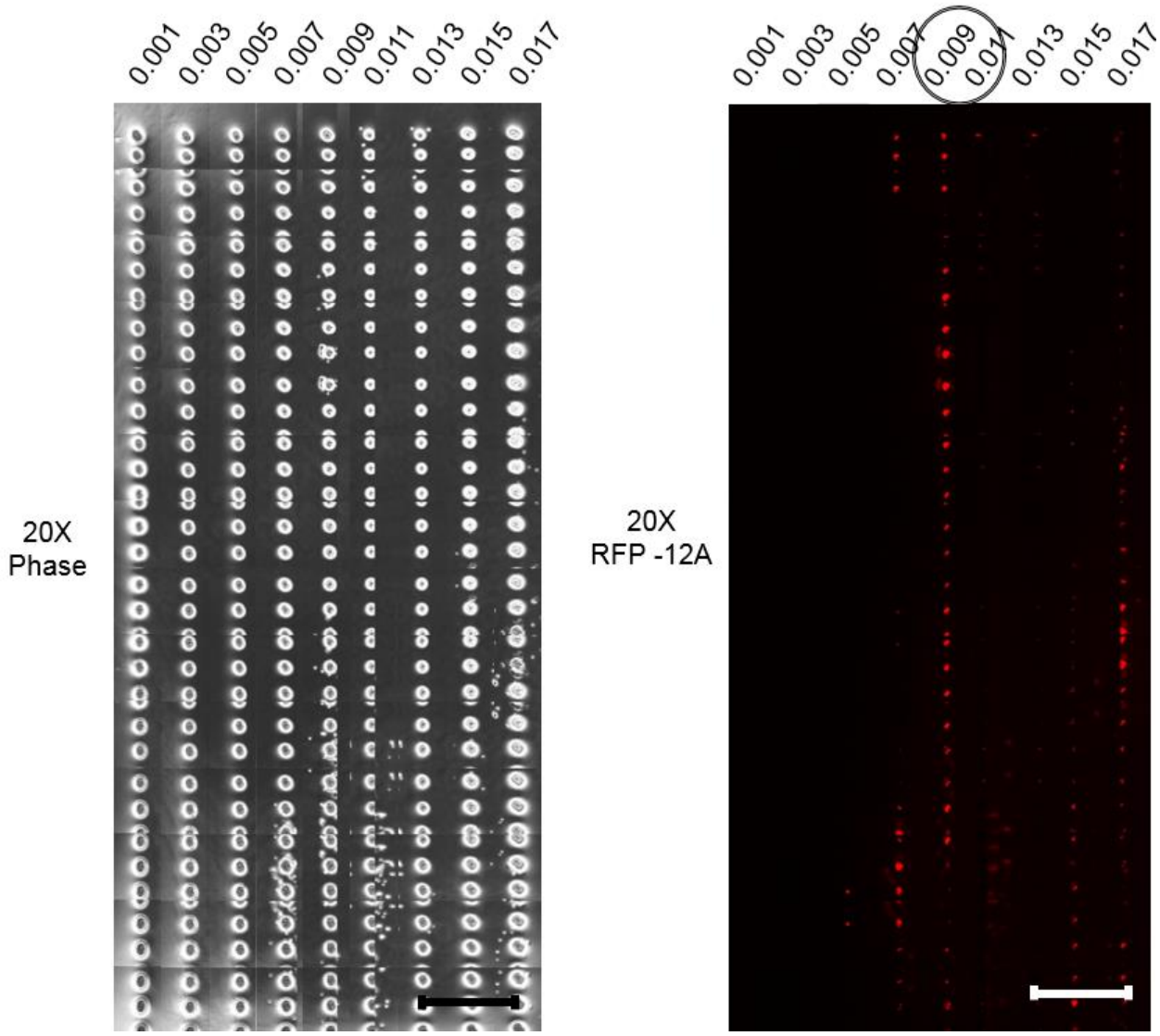

Figure 15. Experimental determination of the most suitable extrusion value to perform single-cell resolution printing of MCF 12A-RFP cells in 1% agarose gel. Phase imaging (A) confirmed the successful performance of uniform injections throughout the printing experiment. Fluorescence imaging (B) showed consistent single-cell printing at extrusion value E=0.009. Size standard was 1000 µm.

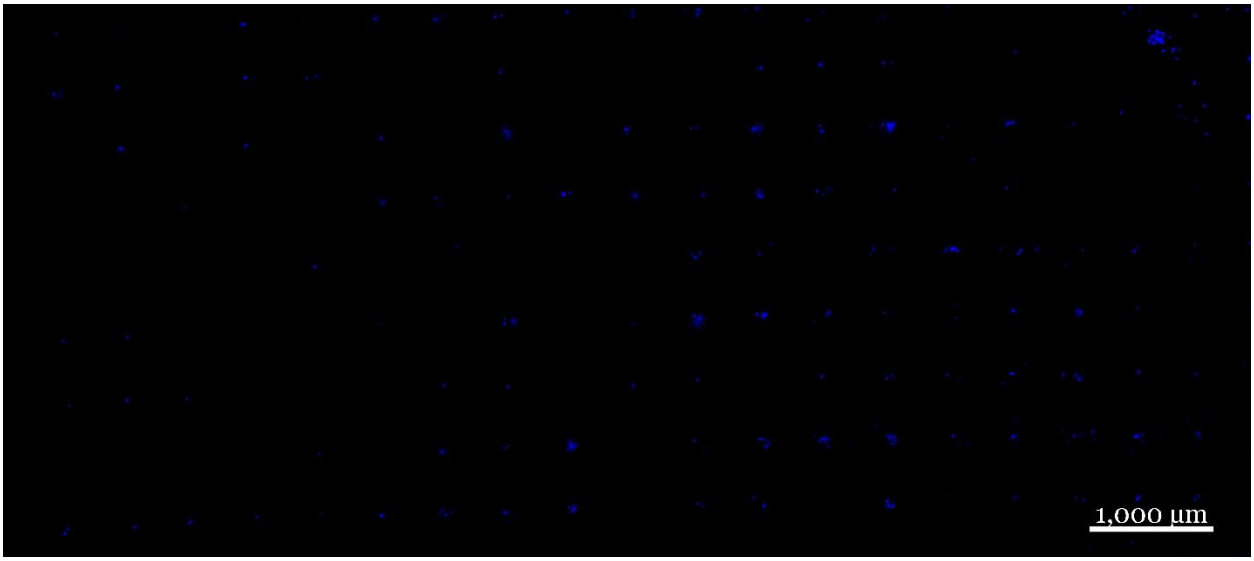

Figure 16. Efficiency of single-cell printing was quantified performing DAPI nuclear staining. Depicted are cells of the MCF7 line printed in 1% agarose gel, with printer parameters set to extrusion value E=0.009 and needle diameter of about 100 µm. Single cells were successfully printed in 35% of the injection sites. Size standard was 1000 µm.

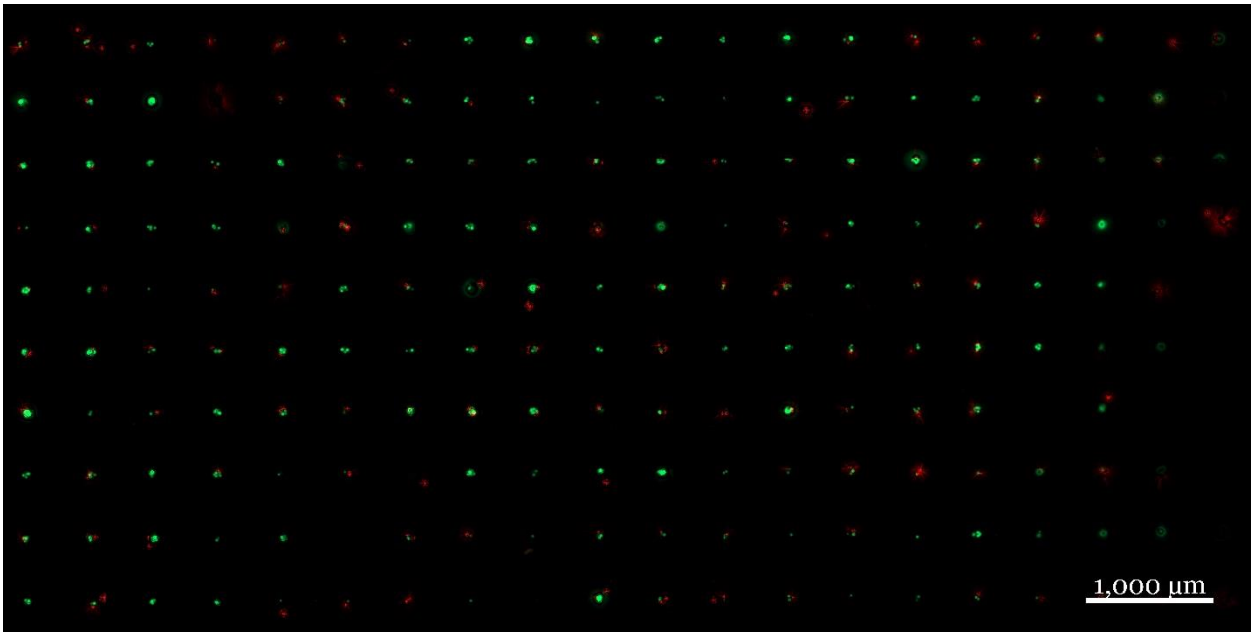

Figure 17. Cells and beads printed on Rat Tail Collagen I gels plated on a PEN membrane, with printer parameters set to extrusion value E=0.009 and needle diameter of about 100 µm. Efficiency of single-cell/single-beads printing was evaluated upon visual inspection of fluorescence images, and 13% of the injections contained one single cell and one single bead. Single cells were printed with an average value of 2 and standard deviation of 1.3, while beads were printed with an average of 0.76 per injection, with a standard deviation value of 0.78. Size standard was 1000 µm.

CHAPTER IV – DISCUSSION

With this project, I developed three separate Aims to establish the foundations of devising a functional three-dimensional cell culture system to be utilized for the study of asymmetrical division using a neural stem cell model. In Aim 1, I adopted a Microelectrode Array system for the study of the physiology of neural stem cells and neurons. In Aim 2, I produced porcine brain-ECM derived hydrogels, suitable for the culture of neural lineage cells. Finally, in Aim 3, I applied a 3D extrusion-based bioprinting system to achieve single-cell/single-beads resolution printing.

c. Aim (1) – Functional Characterization of Neural Stem Cells and Neurons

Fundamental for the development of Aim 1 and for subsequent applications of the 3D culture system, was the creation of neural stem cell lines starting from induced-pluripotent stem cells. After confirmation of pluripotency of the iPSCs populations, wild-type (bASC3.2), Alzheimer's disease (AG09088.1) and Huntington's disease (GM02191.1) neural stem cell lines were successfully induced through the embryoid body method. Identity of the NSC lines and their ability to differentiate into neurons were confirmed through ICC assays and gene expression analysis. Creation of such lines allowed for the correct development of Aim 1, as well as providing a valuable tool for the future application of the optimized 3D cell culture system to the study of asymmetrical cell division and neurological diseases.

Further, I evaluated the suitability of MEA systems to measure the spontaneous electrical activity of neural stem cell and neurons of the lines previously generated. This allows for us to confirm functional characteristics of our neuronal cells. Two different protocols were used, which envisioned coating of the MEA plates with Geltrex® or laminin. It was observed that no significant activity was present from the NSCs of any of the cell lines tested. The absence of activity was

attributed to the nature of the cells in analysis. Neural stem cells are a progenitor cell type, with no recorded data of transmitted electrical signals within the brain. However, patterns of ion-channel presence suggest potential activity may be present, but at decreased magnitudes. Differently, neurons of all the cell lines tested presented discernable electrical activity when plated on laminin-coated MEA plates, while none when plated on Geltrex® matrix. Laminin resulted a more suitable substrate for the purpose, as the characteristic thickness of Geltrex® results in insulation of the recording electrodes, and limited ability to measure changes in voltage from the cell network [47]. The MEA system, with the optimal coating substrate, represented an accessible and efficient methods to study the electrophysiology of neuronal networks. It has the potential to contribute to the elucidation of the changes in neural cells' electrophysiological properties during development and maturation, giving our lab a key method of characterization. Optimization of the MEA plates coating and plating techniques still need to be performed for accurate physiological measurements.

Future Aims include the development and adaptation of a three-dimensional MEA system to an ECM-based culture system. This would allow the performance of real time physiological measurements of the cells under analysis, particularly focusing on the changes in electrophysiology that characterize wild type and diseased neural stem cell lines in a three-dimensional context.

d. Aim (2) – Fabrication of porcine brain matrix-derived hydrogels suitable for cell culture

In Aim 2 I explored the possibility of creating a tissue-specific substrate derived from porcine brain ECM, and evaluated its suitability for neuronal cell culture. The protocol I adopted resulted in the successful generation of a self-gelling product, comparable in protein content to the commercially available Geltrex®, already widely used for 2D and 3D cell culture purposes.

The decellularization protocol adopted was overall effective and the genomic DNA content of the product was reduced by about 65% compared to the brain control. Ideally, gDNA content should be reduced by about 90%, therefore optimization of this protocol is recommended to further decrease the final gDNA content, as well as increasing the final product yield. One potential improvement to the protocol is represented by the adoption of a peristaltic pump system to perform the water, decellularization and sterilizing solution washes. Such system would precisely regulate the flow (force) of incoming washes/treatments, thus preventing the necessity to remove the tissue from its container at every step of the process, reducing the product loss associated with it, as well as the risk of contamination. Additionally, using a peristaltic pump would ensure a continuous flow and replenishment of the solvent. The fluids would then be able to penetrate the tissue even at low flow rates, eliminating the necessity for an orbital shaker and resulting in reduced degeneration of the sample's macroscopic structures. This would ideally lead to an increase in the final product yield and allow for the design of experiments targeting different anatomical regions of the brain.

The brain-derived product was shown to be biocompatible through *in vivo* experiments, and to allow the survival and proliferation of iPSC and NSC over a prolonged time. It can be inferred that the matrix-derived product is therefore suitable for a three-dimensional cell culture system where stem cell lines are injected into the hydrogel. Optimization of our protocol is however needed to render the product suitable for culture ware coating and allow iPSCs and NSCs to attach and expand two-dimensionally on the substrate.

Future developments of this Aim, following the successful optimizations previously mentioned, include the application of the brain-derived substrate for the three-dimensional culture of wild-type, Alzheimer's disease and Huntington's disease iPSC, NSC, and neurons. The

suitability of the substrate for the long-term culture of each cell type shall be tested applying the substrate to coat culture plates, by culturing cells over thin gel layers, by embedding the cells within the substrate prior to plating, and by injecting the cells via 3D bioprinting. The ability of each cell type to survive, proliferate, and differentiate in each environment will be evaluated, and consequently, the suitability of the substrate to enable the study of asymmetrical division of neural stem cell, as well as performance of experiments designed to study the mechanisms of each disease in a three-dimensional setting.

e. Aim (3) – Optimization of a 3D extrusion-based bioprinter to obtain single-cell/single-beads resolution printing.

In the third Aim of this project I adjusted the parameters of a custom 3D extrusion-based bioprinter to obtain single-cell/single-beads printing resolution. Preliminary experiments were performed injecting MCF7, MCF12A, or MDA-MB-468 cells in 1% agarose gels, all materials adopted as they were readily available in our lab and represented a suitable model for neural stem cells injected in ECM based hydrogels. Consistent single-cell resolution prints were obtained setting the printer extrusion value to E=0.009 and fabricating needles of inner diameter between 100-500 µm. Initially we had a large amount of clusters that began to form before printing, making single cell prints difficult. Increased maintenance of a single cell state of the cell in suspension was made possible by resuspension in a chelating agent. This improvement to our protocol made it possible for us to successfully print single cell events 35% of the time.

Subsequent experiments were performed with the goal of achieving single-cell/single-beads resolution printing into Rat Tail Collagen I gels. A success rate of a single cell and a single bead was achieved 13% of the time. This was accomplished by slightly adjusting the cells and

beads concentrations, as well as the needle diameter. Lower precision of the printing, compared to the numbers reported printing single cells on agarose gels, was associated with issues relating to the resuspend cells and beads in a chelating agent prior to printing. In fact, addition of EDTA would have a counterproductive effect in allowing the placement of one cell in contact with one bead, as the agent would act against binding of cells and beads in the same way it interferes in the formation of cell clusters. To increase the efficiency of single-cell and single-bead prints, the parameters of cell concentration, bead concentration, needle-tip diameter, and time-interval between preparation and printing, would require optimization. Such parameters include cells concentration, beads concentration, needle diameter, and interval between cell dilution and printing to prevent cell clusters formation. However, even with a 13% single bead/single cell rate the high-throughput nature of our 3D printing system still was able to achieve ~26 successful events in a 10x20 grid. Not counting the possibility of improving our efficiency, expanded arrays >100x200 are plausible with our system making a 13% success rate a reasonable N for future studies of asymmetric divisions.

Further developments of this Aim include performing cell-bead conjugation prior to their injection in the substrate. This would ensure their contact following printing. Further adjustment of the printing parameters will be necessary to ensure optimal single-cell/single-beads printing resolution using conjugated beads. Finally, the same experiments will be repeated using iPSCs and NSCs conjugated to red Fluoroshperes® beads and Wnt transcription factors, to evaluate the suitability of the system and the previously determined parameters to study the different cell types, and ultimately design experiments for the study of asymmetrical division mechanisms.

The three Aims developed within this project resulted in tangible improvements towards the development of a functional three-dimensional cell culture system for the study of asymmetrical division in neural stem cells. Optimization and further development of each Aim is necessary before experiments culturing and differentiating cells in the 3D culture system can be designed and performed. With this project, concrete steps were taken for the application of MEA systems to perform electrophysiological studies, the development of tissue-specific substrates suitable for stem and neural cell culture, and the application of a 3D extrusion-based for single-cell resolution printing. The foundations for the application of each technique to the development of a sophisticated three-dimensional cell culture system were laid. The scope of the project set the basis for the development of a system to study asymmetrical cell division. However, the finalized system will allow the performance of broader projects, including studies concerning the mechanisms that characterize neurological diseases.

CHAPTER V – REFERENCES

[1] D. L. Myster and R. J. Duronio, "Cell cycle: To differentiate or not to differentiate?," *Current Biology,* vol. 10, no. 8, pp. R302-R304, 2000/04/15/ 2000.

[2] S. Mitalipov and D. Wolf, "Totipotency, pluripotency and nuclear reprogramming," *Adv Biochem Eng Biotechnol,* vol. 114, pp. 185-99, 2009.

[3] S. B. Hima Bindu A, "Potency of Various Types of Stem Cells and their Transplantation," *Journal of Stem Cell Research and Therapy* Review 2011.

[4] P. C. Sachs, P. A. Mollica, and R. D. Bruno, "Tissue specific microenvironments: a key tool for tissue engineering and regenerative medicine," *Journal of Biological Engineering,* vol. 11, p. 34, 11/16

[5] R. D. Bruno and G. H. Smith, "Reprogramming non-mammary and cancer cells in the developing mouse mammary gland," *Seminars in cell & developmental biology,* vol. 23, no. 5, pp. 591-598, 03/10 2012.

[6] J. A. Thomson *et al.*, "Embryonic Stem Cell Lines Derived from Human Blastocysts," *Science,* 10.1126/science.282.5391.1145 vol. 282, no. 5391, p. 1145, 1998.

[7] K. Takahashi *et al.*, "Induction of Pluripotent Stem Cells from Adult Human Fibroblasts by Defined Factors," *Cell,* vol. 131, no. 5, pp. 861-872, 2007.

[8] K. Tanabe, K. Takahashi, and S. Yamanaka, "Induction of pluripotency by defined factors," *Proc Jpn Acad Ser B Phys Biol Sci,* vol. 90, no. 3, pp. 83-96, 2014.

[9] N. Malik and M. S. Rao, "A Review of the Methods for Human iPSC Derivation," *Methods in molecular biology (Clifton, N.J.),* vol. 997, pp. 23-33, 2013.

[10] T. H. Cheung and T. A. Rando, "Molecular regulation of stem cell quiescence," *Nature reviews. Molecular cell biology,* vol. 14, no. 6, p. 10.1038/nrm3591, 2013.

[11] H. Clevers, "What is an adult stem cell?," *Science,* 10.1126/science.aad7016 vol. 350, no. 6266, p. 1319, 2015.

[12] J. Voog and D. L. Jones, "Stem cells and the niche: a dynamic duo," (in eng), *Cell Stem Cell,* vol. 6, no. 2, pp. 103-15, Feb 5 2010.

[13] F. Ferraro, C. L. Celso, and D. Scadden, "ADULT STEM CELLS AND THEIR NICHES," *Advances in experimental medicine and biology,* vol. 695, pp. 155-168, 2010.

[14] J. A. Knoblich, "Mechanisms of Asymmetric Stem Cell Division," *Cell,* vol. 132, no. 4, pp. 583-597, 2008.

[15] K. Duval *et al.*, "Modeling Physiological Events in 2D vs. 3D Cell Culture," *Physiology,* vol. 32, no. 4, pp. 266-277, 06/14

[16] A. Khoruzhenko, *2D- and 3D-cell culture*. 2011, pp. 17-24.

[17] T. Hartung, "Thoughts on limitations of animal models," *Parkinsonism & Related Disorders,* vol. 14, pp. S81-S83, 2008/07/01/ 2008.

[18] M. Jucker, "The benefits and limitations of animal models for translational research in neurodegenerative diseases," *Nature Medicine,* vol. 16, p. 1210, 09/21/online 2010.

[19] R. Maddaly, P. V., K. S.R., A. E., and S. F. D. Paul, "3D Cell Culture Systems: Advantages and Applications," *Journal of Cellular Physiology,* vol. 230, no. 1, pp. 16-26, 2015.

[20] R. Edmondson, J. J. Broglie, A. F. Adcock, and L. Yang, "Three-Dimensional Cell Culture Systems and Their Applications in Drug Discovery and Cell-Based Biosensors," *Assay and Drug Development Technologies,* vol. 12, no. 4, pp. 207-218, 2014.

[21] J. G. Webster, *Medical Intrumentation. Application and Design*, Fourth ed. Wiley, 2010.

[22] J. Malmivuo and R. Plonsey, *Bioelectromagnetism - Principles and Applications of Bioelectric and Biomagnetic Fields*. 1995.

[23] A. Odawara, Y. Saitoh, A. H. Alhebshi, M. Gotoh, and I. Suzuki, "Long-term electrophysiological activity and pharmacological response of a human induced pluripotent stem cell-derived neuron and astrocyte co-culture," *Biochem Biophys Res Commun,* vol. 443, no. 4, pp. 1176-81, Jan 24 2014.

[24] H. Amin, A. Maccione, F. Marinaro, S. Zordan, T. Nieus, and L. Berdondini, "Electrical Responses and Spontaneous Activity of Human iPS-Derived Neuronal Networks Characterized for 3-month Culture with 4096-Electrode Arrays," (in English), *Frontiers in Neuroscience,* Original Research vol. 10, no. 121, 2016-March-30 2016.

[25] H. C. S., P. L. M., and L. G. A., "Matrigel: A complex protein mixture required for optimal growth of cell culture," *PROTEOMICS,* vol. 10, no. 9, pp. 1886-1890, 2010.

[26] S. H. Choi *et al.,* "A three-dimensional human neural cell culture model of Alzheimer's disease," *Nature,* vol. 515, no. 7526, pp. 274-8, Nov 13 2014.

[27] W. Yan *et al.,* "A Three-Dimensional Culture System with Matrigel Promotes Purified Spiral Ganglion Neuron Survival and Function In Vitro," *Mol Neurobiol,* Mar 10 2017.

[28] G. Sun *et al.,* "The Three-Dimensional Culture System with Matrigel and Neurotrophic Factors Preserves the Structure and Function of Spiral Ganglion Neuron In Vitro," *Neural Plast,* vol. 2016, p. 4280407, 2016.

[29] E. Polykandriotis, A. Arkudas, R. E. Horch, U. Kneser, and G. Mitchell, "To Matrigel or Not to Matrigel," *The American Journal of Pathology,* vol. 172, no. 5, pp. 1441-1442, 2008/05/01/ 2008.

[30] R. D. Bruno, J. M. Fleming, A. L. George, C. A. Boulanger, P. Schedin, and G. H. Smith, "Mammary extracellular matrix directs differentiation of testicular and embryonic stem cells to form functional mammary glands in vivo," *Sci Rep,* vol. 7, p. 40196, Jan 10 2017.

[31] J. A. DeQuach, S. H. Yuan, L. S. Goldstein, and K. L. Christman, "Decellularized porcine brain matrix for cell culture and tissue engineering scaffolds," *Tissue Eng Part A,* vol. 17, no. 21-22, pp. 2583-92, Nov 2011.

[32] P. M. Crapo *et al.*, "Biologic scaffolds composed of central nervous system extracellular matrix," *Biomaterials,* vol. 33, no. 13, pp. 3539-47, May 2012.

[33] C. J. Medberry *et al.*, "Hydrogels derived from central nervous system extracellular matrix," *Biomaterials,* vol. 34, no. 4, pp. 1033-40, Jan 2013.

[34] A. R. John, A. M. Peter, D. J. Garett, C. O. Roy, D. B. Robert, and C. S. Patrick, "Accessible bioprinting: adaptation of a low-cost 3D-printer for precise cell placement and stem cell differentiation," *Biofabrication,* vol. 8, no. 2, p. 025017, 2016.

[35] S. J. Habib *et al.*, "A Localized Wnt Signal Orients Asymmetric Stem Cell Division in Vitro," *Science (New York, N.Y.),* vol. 339, no. 6126, pp. 1445-1448, 2013.

[36] P. A. Mollica *et al.*, "Epigenetic alterations mediate iPSC normalization of DNA-repair expression and TNR stability in Huntington's disease," *Journal of Cell Science,* 10.1242/jcs.215343 2018.

[37] J. T. Dimos *et al.*, "Induced Pluripotent Stem Cells Generated from Patients with ALS Can Be Differentiated into Motor Neurons," *Science,* 10.1126/science.1158799 vol. 321, no. 5893, p. 1218, 2008.

[38] M. Ehrlich *et al.*, "Rapid and efficient generation of oligodendrocytes from human induced pluripotent stem cells using transcription factors," *Proceedings of the National Academy of Sciences of the United States of America,* vol. 114, no. 11, pp. E2243-E2252, 02/28 2017.

[39] S. Derakhshanfar, R. Mbeleck, K. Xu, X. Zhang, W. Zhong, and M. Xing, "3D bioprinting for biomedical devices and tissue engineering: A review of recent trends and advances," *Bioactive Materials,* vol. 3, no. 2, pp. 144-156, 2018/06/01/ 2018.

[40] D. Pozzi, J. Ban, F. Iseppon, and V. Torre, "An improved method for growing neurons: Comparison with standard protocols," *Journal of Neuroscience Methods,* vol. 280, pp. 1-10, 2017/03/15/ 2017.

[41] S. Sinha and J. K. Chen, "Purmorphamine activates the Hedgehog pathway by targeting Smoothened," *Nature Chemical Biology,* vol. 2, p. 29, 11/20/online 2005.

[42] A. W. Janesick, S. C. , "Retinoic acid signaling and neuronal differentiation.," *Cellular and Molecular Life Sciences,* vol. 72, no. 8, pp. 1559-1576, 2015.

[43] T. Cho *et al.,* "Human neural stem cells: electrophysiological properties of voltage-gated ion channels," *Neuroreport,* vol. 13, no. 11, pp. 1447-52, Aug 7 2002.

[44] E. Ruoslahti, "Brain extracellular matrix," (in eng), *Glycobiology,* vol. 6, no. 5, pp. 489-92, Jul 1996.

[45] A. Wade, A. E. Robinson, J. R. Engler, C. Petritsch, C. D. James, and J. J. Phillips, "Proteoglycans and their roles in brain cancer," *The FEBS journal,* vol. 280, no. 10, pp. 2399-2417, 02/06 2013.

[46] C. Frantz, K. M. Stewart, and V. M. Weaver, "The extracellular matrix at a glance," *Journal of Cell Science,* vol. 123, no. 24, pp. 4195-4200, 12/01 2010.

[47] P. K. LaFosse *et al.,* "Effect of substrate coating material on spontaneous activity of human-induced pluripotent stem cell-derived neuronal stem cells," (in English), *Frontiers in Cellular Neuroscience,* Abstract.

Vita

Martina Zamponi was born in the city of Moncalieri (TO), Italy. In 2014, she moved to Virginia Beach, VA, where she completed her high school education. She then attended Old Dominion University and completed her B.S. in Biology with minor in Biomedical Engineering in 2017. At the same university, she attended graduate school to earn her M.S. in Biomedical Engineering in 2018. She plans to continue her studies and research in the field of Biomedical Engineering.